remote sensing

MDPI

Article

Detection, Localization and Classification of Multiple Mechanized Ocean Vessels over Continental-Shelf Scale Regions with Passive Ocean Acoustic Waveguide Remote Sensing

Chenyang Zhu [1], Heriberto Garcia [1], Anna Kaplan [1], Matthew Schinault [1], Nils Olav Handegard [2], Olav Rune Godø [3], Wei Huang [1] and Purnima Ratilal [1,*]

[1] Department of Electrical and Computer Engineering, Northeastern University, 360 Huntington Ave, Boston, MA 02115, USA; zhu.che@husky.neu.edu (C.Z.); garcia.he@husky.neu.edu (H.G.); kaplan.ann@husky.neu.edu (A.K.); schinault.m@husky.neu.edu (M.S.); huang.wei1@husky.neu.edu (W.H.)
[2] Institute of Marine Research, Post Office Box 1870, Nordnes, N-5817 Bergen, Norway; nilsolav@imr.no
[3] Christian Michelsen Research AS, Fantoftvegen 38, 5072 Bergen, Norway; olav.rune.godoe@imr.no
* Correspondence: purnima@ece.neu.edu; Tel.: +1-617-373-8458

Received: 10 September 2018; Accepted: 19 October 2018; Published: 29 October 2018

Abstract: Multiple mechanized ocean vessels, including both surface ships and submerged vehicles, can be simultaneously monitored over instantaneous continental-shelf scale regions >10,000 km^2 via passive ocean acoustic waveguide remote sensing. A large-aperture densely-sampled coherent hydrophone array system is employed in the Norwegian Sea in Spring 2014 to provide directional sensing in 360 degree horizontal azimuth and to significantly enhance the signal-to-noise ratio (SNR) of ship-radiated underwater sound, which improves ship detection ranges by roughly two orders of magnitude over that of a single hydrophone. Here, 30 mechanized ocean vessels spanning ranges from nearby to over 150 km from the coherent hydrophone array, are detected, localized and classified. The vessels are comprised of 20 identified commercial ships and 10 unidentified vehicles present in 8 h/day of Passive Ocean Acoustic Waveguide Remote Sensing (POAWRS) observation for two days. The underwater sounds from each of these ocean vessels received by the coherent hydrophone array are dominated by narrowband signals that are either constant frequency tonals or have frequencies that waver or oscillate slightly in time. The estimated bearing-time trajectory of a sequence of detections obtained from coherent beamforming are employed to determine the horizontal location of each vessel using the Moving Array Triangulation (MAT) technique. For commercial ships present in the region, the estimated horizontal positions obtained from passive acoustic sensing are verified by Global Positioning System (GPS) measurements of the ship locations found in a historical Automatic Identification System (AIS) database. We provide time-frequency characterizations of the underwater sounds radiated from the commercial ships and the unidentified vessels. The time-frequency features along with the bearing-time trajectory of the detected signals are applied to simultaneously track and distinguish these vessels.

Keywords: passive ocean acoustic waveguide remote sensing; multiple ships; ship noise; tonal; ship detection; localization; classification; beamforming; triangulation; hydrophone array; passive acoustics

1. Introduction

Here we demonstrate the instantaneous wide-area monitoring of multiple mechanized ocean vessels over 10,000 km^2 region present in two days of Passive Ocean Acoustic Waveguide Remote

Sensing (POAWRS) during Spring 2014 in the Norwegian Sea. A large-aperture densely-sampled coherent hydrophone array system with 160-elements was deployed to record the underwater sound radiated from a large variety of oceanic sound sources [1,2]. The hydrophone array provides directional sensing in a 360-degree horizontal azimuth via coherent beamforming of the recorded underwater acoustic data. The POAWRS technique [2–7] is employed here to provide detection, localization and classification of mechanized ocean vessels from their underwater sounds received on the coherent hydrophone array. Between 10 to 25 distinct mechanized ocean vessels could be detected and tracked in roughly 8 h of POAWRS observation per day. The underwater sounds radiated from the mechanized ocean vessels were detected with significantly high Signal-to-Noise Ratios (SNR) after coherent beamforming of the acoustic data received on the hydrophone array, leading to detection ranges that are up to two orders of magnitude more distant than that for a single hydrophone [2].

Our approach for POAWRS monitoring of ocean vessels from their underwater sounds measured on a coherent hydrophone array follows that of Ref. [2] where the method was previously developed and calibrated for three known mechanized surface ships that are powered by either diesel or diesel-electric engines. They are Research Vessel (RV) Delaware II in the Gulf of Maine, RV Johann–Hjort and Fishing Vessel (FV) Artus in the Norwegian Sea. The Global Positioning System (GPS) measured latitude-longitude locations, available at high sample rate (1 s update), for each of these surface ships were utilized to extract the underwater sounds received by the coherent hydrophone array system. The ranges of the three ships from the coherent hydrophone array varied between 4.8 km to 31 km in the observation time period analyzed in Ref. [2]. The underwater sound received from each of the three ships was found to be dominated by multiple distinct narrowband signals in the 100 Hz to 2 kHz frequency range that are either constant frequency tonals or have frequencies that waver or oscillate slightly in time [2]. The source level of the dominant narrowband signals radiated by each of these three ships were estimated in Ref. [2] and applied to determine the Probability of Detection (PoD) region in the Gulf of Maine or Norwegian Sea environment where the passive acoustic data were acquired. It was found that the 50% PoD region for the passive acoustic detection of these ships can extend roughly 100 km to 200 km from the coherent hydrophone array [2] when propagation conditions are favorable. In general, the passive acoustic detection of ocean vessels with a coherent hydrophone array is dependent on signal source level, frequency, bandwidth, array beamwidth and bearing, as well as environmental ambient noise level and propagation conditions such as bathymetry, water column and sea floor sound speed.

Here, in order to simultaneously monitor the mechanized ocean vessels in a 360-degree horizontal azimuth about the coherent hydrophone array, we first extract signals that follow well-defined bearing-time trajectories dominated by narrowband signals that are either constant frequency tonals or have frequencies that waver or oscillate slightly over time, since these signals are characteristic of mechanized ocean vessels. We then cluster these signals and associate them with distinct ocean vessels using their time-frequency characteristics and their bearing-time trajectories. Each ocean vessel is next localized from its corresponding bearing-time trajectory of signal detections employing the Moving Array Triangulation (MAT) [8] technique. Of the 30 mechanized ocean vessels detected in roughly 8 h observation time interval per day for two days, 20 of these could be identified as named commercial ships since their bearing-time trajectories and locations correspond well with those derived from GPS records in the satellite or terrestrial based Automatic Identification System (AIS) historical database of the region for these days. The remaining 10 ocean vessels could not be identified because of sparse or absent GPS information in the historical AIS database during the operation time of our array making it challenging to associate them with detected ocean vessels in our dataset.

The remote monitoring of ocean vessels over instantaneous wide areas from their sounds radiated underwater is essential in maritime surveillance and defence. The sound generated by ocean vessels contributes to environmental ambient noise [9] and sets limiting ranges for detection in both passive and active sonar systems for a wide range of ocean remote sensing applications, as well as in man-made communication systems [10,11]. The vessel generated noise may also influence

behavior of marine organisms [9,12–14], such as fish [15–18] and marine mammals [19–21]. Signals generated by mechanized vessels form important components of the soundscape [22–24] in most ocean environments.

Passive acoustic methods have been previously used to examine, characterize and quantify the sound radiated from ocean vessels. The majority of measurements in published literature is obtained using a single hydrophone [25,26] or a small number of widely-separated hydrophones [27–29] located within a few hundred meters to a few kilometers from a ship. Ship-radiated sound has also been measured using a 128-element vertical hydrophone array [30] and bottom-mounted hydrophones [31]. In addition to SNR enhancement, an advantage of using a coherent hydrophone array, such as the one used here, is that the bearing of the sound radiated by the vessel can be estimated and tracked over time [2]. This bearing-time trajectory of signal detections from a given vessel can be employed for estimating the horizontal position of the vessel in geographic space. In contrast, single hydrophone or sparse array measurements lead to low SNR in detections of a vessel's underwater radiated sound, poor or no angular resolution to discriminate the direction of the sound sources, and significantly limited vessel detection ranges.

The mechanism of sound generation by ships is described in [32–39], with the main sources arising from machinery noise generated by propulsion and machinery such as engines, main motors and gears; propeller noise generated by cavitation at or near the propeller and propeller-induced resonant hull excitation; hydrodynamic noise from radiated flow noise, resonant excitation of cavities, plates, and appendages; and cavitation at struts and appendages. Ship noise has been previously found to be dominated by propeller cavitation, propeller singing due to physical excitation at the trailing edges of the blades, and propulsion or other reciprocating machinery.

Here we provide the time-frequency characteristics of the dominant narrowband signals received from each of the 30 distinct ocean vessels detected at varying ranges from roughly 5 km to over 150 km from the coherent hydrophone array (Tables 1–4). These characteristics can be employed in future automatic classification systems for potential real-time passive acoustic identification of ocean vessels. The general analysis of ship-generated underwater sound and their characteristics can also be used to improve ship design [2,17,18] to make them quieter, thereby reducing the overall ship radiated noise in the ocean.

2. Methods

2.1. Experiment

Our analysis here is based on a subset of data acquired in the Norwegian Sea 2014 Experiment (NorEx14) [1,2] from 18 February to 7 March in 2014, which was conducted by a collaborative team from the Massachusetts Institute of Technology, Northeastern University, NOAA-Northeast Fisheries Science Center, Naval Research Laboratory, Penn State University, and Woods Hole Oceanographic Institution in the US, as well as The Institute of Marine Research-Bergen in Norway. A map of the Norwegian coastline along with the data collection regions is provided in Figure 1 of Ref. [1]. During this experiment, a large aperture, densely-sampled coherent horizontal hydrophone array was towed at an average speed of four knots or roughly 2 m/s along designated tracks for 8 to 24 h per day to record underwater sound. To minimize the effect of tow ship noise (refer to Appendix A) on the recorded acoustic data, the coherent hydrophone array was towed approximately 280 m to 330 m behind the research vessel so as to confine this noise to the forward endfire direction of the array, which is the forward direction parallel to the array axis. The water depth ranged from 100 m to 300 m at the array locations, and the array tow depth varied between 45 m to 70 m.

2.2. Hydrophone Array

The hydrophone array we utilized during the experiment contains 160 hydrophones [40] which are nested into multiple sub-apertures spanning a frequency range from below 10 Hz to 4 kHz for

spatially unaliased sensing [41]. The sampling frequency is set to be 8 kHz to ensure temporally unaliased sensing up to 4 kHz [42]. Three linear nested sub-apertures of the array were used to analyze ship-radiated sound: the ultra low-frequency (ULF), mid-frequency (MF) and high-frequency (HF) sub-apertures, each consisting of 64 equally spaced hydrophones with inter-element spacings of 3 m, 0.75 m, and 0.375 m, respectively. Detailed geometry and design criteria for the coherent hydrophone array deployed in this experiment are provided and discussed in Refs. [40,43].

The detection of long-range propagated sounds is significantly enhanced by spatial beamforming and spectrogram analysis which filters the background noise that is outside of the beam and frequency band of the ship-radiated sound. The high gain of the large aperture densely-sampled coherent hydrophone array used here, roughly $10log_{10}(n) = 18$ dB gain with $n = 64$ hydrophones for each sub-aperture, enabled detection of continuous tonal noises up to two orders of magnitude more distant in range or lower in SNR than a single hydrophone which has no array gain (see Figure 2 of [2]). The actual array gain, which may be smaller than the full 18-dB theoretical array gain, is dependent on noise coherence and signal wavelength relative to array aperture length. The horizontal azimuthal spatial filtering provided by the linear array used here is quantified by the beampattern of the array. The beamforming technique constructively adds plane wave arrivals in the steering or look direction of the array leading to a peak in the beampattern. Plane wave arrivals away from the steering direction add non-constructively or even destructively to create nulls in the beampattern. The horizontal beamwidth of the array is a function of the array aperture length L, steering angle ϕ, as well as center frequency f_c and bandwidth B of the signal [41,44,45]. As an example, the 1 dB angular width $\beta_{1dB}(\phi, f_c)$ [7] of the receiver array at 130 Hz is approximately 1.7 degrees. A Hanning spatial window is applied in the beamforming.

Physical oceanography was monitored by sampling water-column temperature and salinity with expendable bathythermographs (XBTs) and conductivity-temperature-depth (CTD) sensors at regular intervals of a couple of hours each day. The water-column sound speed profile measured in the Norwegian Sea are provided in [46] along with an analysis of the range- and depth-dependent transmission loss for a variety of source-receiver geometries and transects in this environment. The empirically determined acoustic ambient noise spectral density levels based on measurements in the Norwegian Sea are provided in Table A1 of Ref. [2] and Table 5 of Ref. [1] at a range of frequencies from 20 Hz to 1800 Hz.

The POAWRS coherent hydrophone array employed in NorEx14 detected significant sounds from a wide range of underwater acoustic sources including marine mammal vocalisations from diverse baleen [1] and toothed whale species in the frequency range from 10 Hz up to 4 kHz, and sounds from a large number of mechanized surface ships and other ocean vessels [2]. Here the analysis is focused on the simultaneous detection and characterization of multiple mechanized ocean vessels between the 10 Hz to 4000 Hz frequency range.

2.3. Signal Detection and Clustering

Acoustic pressure time series measured by sensors across the receiver array were converted to two-dimensional beam-time series by beamforming. A total of 64 beams were formed spanning 360-degree horizontal azimuth about the receiver array for data from each subaperture. Each beam-time series was converted to a beamformed spectrogram by short-time Fourier transform (sampling frequency = 8000 Hz, frame = 2048 (ULF), 1024 (MF) and 516 (HF) samples, overlap = 15/16, Hann window). Significant sounds present in the beamformed spectrograms were automatically detected by first applying a pixel intensity threshold detector [47] followed by pixel clustering, and verified by visual inspection. The beamformed spectrogram background time-frequency pixel can be treated as instantaneous with time-bandwidth product μ =1 and 5.6 dB intensity standard deviation [1,4,48,49]. Beamformed spectrogram pixels with local intensity values that are 10 dB or roughly two standard deviations above the background are grouped using a clustering algorithm according to a nearest-neighbour criteria that determines if the pixels can be grouped into one or

more significant sound signals. Note that the detection threshold used is highly dynamic since the background ambient noise levels in the beamformed spectrograms are dependent on measurement time period, frequency and bearing. The background ambient noise levels are estimated using beamformed spectrogram data segments that are devoid of ship-radiated signals and other significant sound sources.

Each detected signal is next characterized by its pitch track [2,4,50,51] representing the time variation of the fundamental frequencies. The pitch track is estimated using a time-frequency peak detector from a signal's detected and clustered pixel intensity values in the beamformed spectrogram [2].

The horizontal azimuthal direction or bearing $\hat{\phi}$ of each detected signal, measured from array broadside, is estimated using a beamforming technique [41] that selects the bearing in which the beamformed, band-pass filtered pressure- time series contained maximum energy during the time duration of the signal and in the same frequency band. The estimated relative bearings $\hat{\phi}$, measured with respect to array broadside, are then converted to absolute bearings, measured from the array centre with respect to true North.

The bearing and time of all detected signals are next analyzed to extract those corresponding to mechanized ocean vessels. The ship-radiated narrowband signals are typically present almost continuously over long time durations in the beamformed spectrograms, so that the signal detections are temporally dense along bearing-time trajectories corresponding to ships. In contrast, the signal detections tend to be less dense in bearing-time trajectories corresponding to natural oceanic sound sources. By setting a threshold on detected signal density, the bearing-time trajectories corresponding to ships are extracted and the associated pitch-tracks verified by visual inspection. Multiple ships are distinguished using the detected signal bearing-time trajectory information combined with cluster analysis of features [2] extracted from the detected signal pitch track: (1) minimum frequency (Hz), f_L; (2) maximum frequency (Hz), f_U; (3) amplitude weighted average frequency (Hz), $\overline{f}$; (4) mean instantaneous bandwidth (Hz), $\overline{B}$; (5) relative instantaneous bandwidth, $\overline{B}/\overline{f}$; (6) duration ($s$), $\tau = t_i - t_1$; (7) slope from first order polynomial fit (Hz/s), $\frac{df}{d\tau}$; and (8) curvature from second order polynomial fit (Hz/s^2), $\frac{d^2f}{d\tau^2}$. The slope and curvature are obtained from second order non-linear curve-fit to the vocalisation traces obtained via pitch-tracking [2]. A combination of k-means [52] and Gaussian Mixture Model (GMM) cluster analysis [53] approaches are employed [4,5]. The POAWRS array processing scheme is depicted in Figure 1.

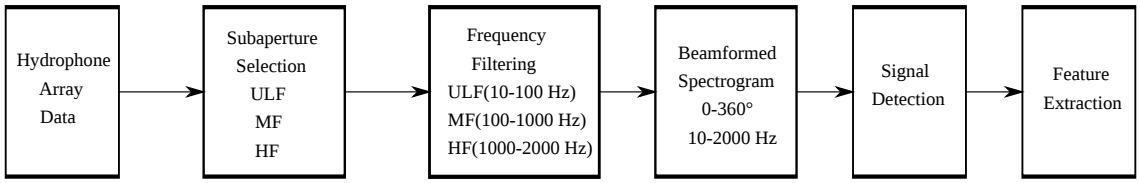

Figure 1. Passive Ocean Acoustic Waveguide Remote Sensing (POAWRS) automated coherent hydrophone array processing scheme.

2.4. Localization

Then, horizontal position of each ocean vessel is estimated from the bearing-time trajectory of corresponding signal detections using bearing-only tracking and localization methods. Here, two localization methods are employed to localize and track the detected ships, the regular MAT technique and the Minimum Mean Square Error implementation of MAT (MAT-MMSE) [8,54]. The MAT technique combines bearing measurements made on adjacent or widely separated finite apertures of a single towed receiver array and employs the conventional triangulation ranging algorithm for localizing sources located in the near- or far-field of the receiver array. At each time instance, the source range is determined as the third point of a triangle from the intersection of the straight lines from pairs of source bearing estimates. This process is repeated for every adjacent

pair of source bearing estimates to provide range estimates. Finally, the sequential source range estimates are mapped onto a Cartesian grid and averaged over a running window to predict the source horizontal trajectory [8]. The MAT-MMSE technique is also based on triangulation but combines sequential bearing measurements in a global inversion for the mean source position over the measurement time interval [8]. The accuracy of the localization result is quantified by the normalized bias: $\epsilon = \frac{|\hat{\bar{r}}_s - \bar{r}_s|}{\overline{R_s}} = \frac{1}{\overline{R_s}}\sqrt{(\hat{\bar{x}}_s - \bar{x}_s)^2 + (\hat{\bar{y}}_s - \bar{y}_s)^2}$, where $\hat{\bar{r}}_s = (\hat{\bar{x}}_s, \hat{\bar{y}}_s)$ is the estimated mean horizontal location, $\bar{r}_s = (\bar{x}_s, \bar{y}_s)$ is the GPS-measured mean horizontal location and $\overline{R_s}$ is the mean range of the localized target from the receiver array.

Position estimation error, or the root-mean-square (RMS) distance between the actual and estimated location, is a combination of range and bearing errors. Bearing estimation error of the beamformer is a function of signal center frequency, bandwidth, and array aperture length. It ranges from roughly 0.5–3 degrees at broadside and gradually increases to 6–10 degrees at endfire. The range estimation error, expressed as the percentage of the range from the source location to the horizontal receiver array centre, has been quantified for this array and broadband signals with roughly 5% bandwidth to centre frequency ratios and approximately 50% centre frequency to array aperture design frequency ratios. In the MAT and MMSE techniques, the range estimation error is roughly 2% at array broadside and gradually increases to 10% at 65° from broadside and 25% near or at endfire [6,8,54]. These errors are determined previously from thousands of controlled broadband source signals transmitted by a source array, and are based on absolute global positioning system (GPS) ground truth measurements of the source array's position [6,8,54]. The position estimation error in the MAT-MMSE technique determined here for the ship radiated narrowband signals from the known ships on 23 February 2014 is 16% after averaging the results over a range of ship speeds and bearings (Tables 1 and 5).

Temperature and salinity perturbations in the water column lead to perturbations in the sound speed. The sound speed perturbations have an insignificant effect on the beamformer output or bearing estimation since the sound speed perturbations are typically small compared to the mean sound speed used in the calculations. The sound speed perturbations also have an insignificant effect on the range estimations since they are based on bearing measurements only.

3. Results

Here we provide detailed analysis of 14 ocean vessels detected by the coherent hydrophone array off the Lofoten archipelago of the Norwegian coast (region II in Figure 1 of Ref. [1]) on 23 February 2014. We first provide the bearing-time trajectories of the detected signals from these vessels against the backdrop of all detections for the day in three distinct frequency subbands, 10–200 Hz, 200–1000 Hz and 1000–2000 Hz, processed using the ULF, MF and HF subapertures, respectively. The mean horizontal positions of the detected vessels estimated using the MAT-MMSE technique are next provided on a geographic map. For the identified commercial ships, their true mean positions based on GPS measurements are also indicated for comparison. Detailed time-frequency properties of the recorded sounds, including spectrograms and pitch-tracks, are provided as examples for two of the 5 identified commercial ships, and two out of nine unidentified vessels. Finally, the characteristics of the dominant narrowband signals received from each of the 14 vessels are summarized in Tables 1 and 2. Similar analysis is applied to acoustic data acquired by the coherent hydrophone array off the northern Finnmark region (region III in Figure 1 of Ref. [1]) of the Norwegian coast on 26 February 2014. The bearing-time trajectories of detected signals from 15 identified commercial ships and 1 unidentified ocean vessel are provided along with a summary of the time-frequency characteristics of the prominent narrowband signals in Tables 3 and 4. Time-frequency characteristics of the tow ship generated noise are provided in the Appendix A for comparison.

3.1. Simultaneous Passive Acoustic Detection and Localization of Multiple Ocean Vessels on 23 February off Lofoten Archipelago

The bearing and time of all detected acoustic signals in the 10 Hz to 2000 Hz frequency range that stand at least 10 dB above the local ambient background noise in the beamformed spectrograms of 23 February 2014 are displayed as gray dots in Figure 2A–C. In each of the three frequency subbands, there are more than 180,000 signal detections in the roughly 8 h observation time interval. In addition to sounds radiated by ocean vessels, the signal detections include marine mammal vocalizations [1], sounds from fish and other ocean biology, as well as other either made-made or natural acoustic and seismic sources. The signal detections from the 14 vessels shown in color, follow distinct and well-defined bearing-time trajectories. Of the 14 vessels detected using passive acoustics, five are identified as commercial ships and labeled as M1, M5, M11, M13 and M14 with names provided in Table 1. For these commercial ships, their bearing-time trajectories and positions derived from the coherent hydrophone array data match well with those derived from GPS measurements of the ships' positions. The remaining nine vessels are unidentified since they could not be associated with other known ships in the region for the day. They are labelled as U2, U3, U4, U6, U7, U8, U9, U10 and U12 in Figure 2A–C and Table 2. These vessels either have sparse or absent GPS information in the historical AIS database to enable identification or confident association with passive acoustic detections.

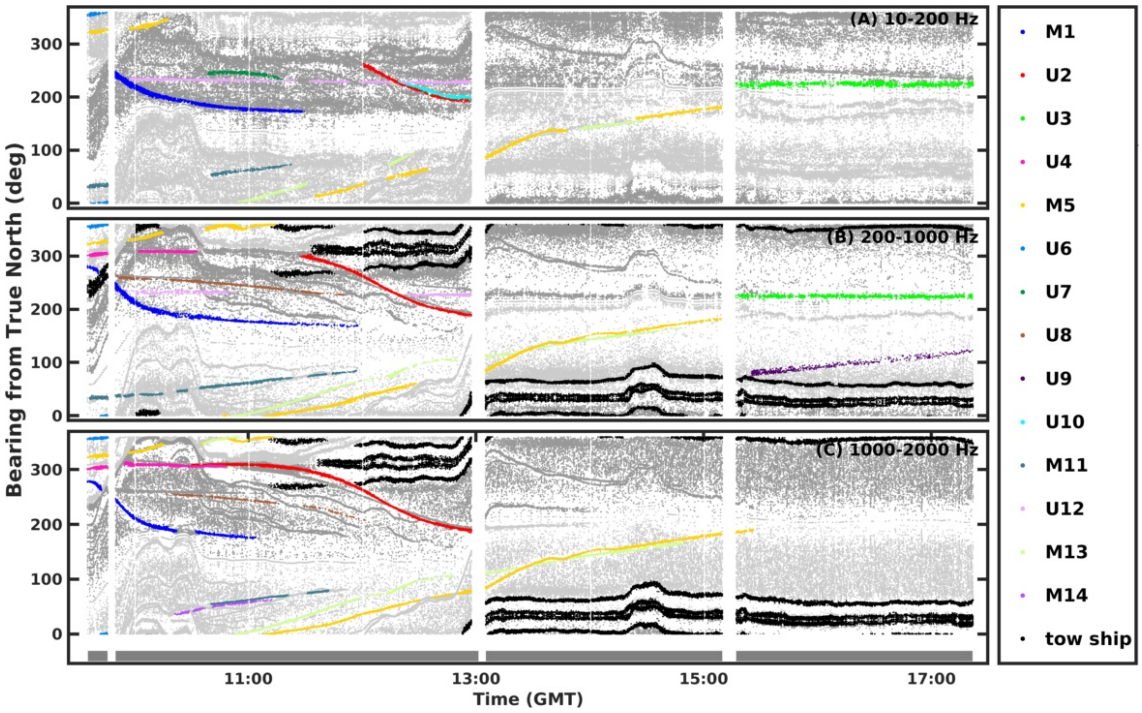

Figure 2. Extracting signal detections from multiple mechanized ocean vessels on 23 February 2014 off the Lofoten archipelago in the (**A**) 10–200 Hz; (**B**) 200–1000 Hz; and (**C**) 1000–2000 Hz frequency subbands. The bearing and time of all detected signals are indicated in gray, spanning 360-degree horizontal azimuth about the coherent hydrophone array from true north. Light and dark gray dots correspond to right and left side bearings, respectively, for all detections about the receiver array, before the line array's left-right bearing ambiguity resolution [8]. Chromatic dots represent signals generated by multiple vessels. The vessels with labels M1, M5, M11, M13 and M14 have been identified as commercial ships (refer to Table 2 for ship name), while vessels with labels U2, U3, U4, U6, U7, U8, U9, U10 and U12 have not been identified. The black dots correspond to signals radiated by the tow ship (see Appendix A). The light gray bar at the bottom shows the coherent hydrophone array recording time intervals.

To localize the ocean vessels from their acoustic signal detections, the bearing-time trajectories of the detected signals are divided into 6 non-overlapping time segments and a mean position estimate is obtained for each vessel present in that time segment using the MAT-MMSE method and plotted in Figures 3 and 4. Twelve of the passively detected ocean vessels are present within 30 km range of the hydrophone array, and three vessels are distant, more than 150 km away.

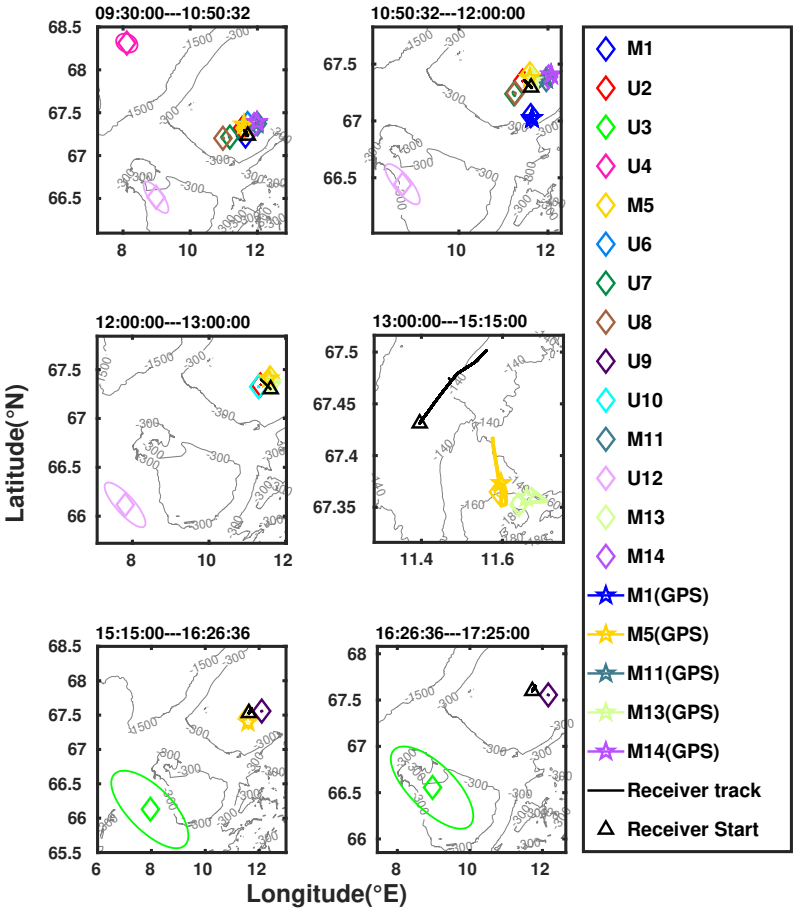

Figure 3. Localization map for all mechanized ocean vessels detected by the coherent hydrophone array on 23 February 2014 off the Lofoten archipelago. Chromatic diamonds indicate mean horizontal position of vessels estimated using the the Minimum Mean Square Error implementation of Moving Array Triangulation (MAT-MMSE) technique in six non-overlapping observation time periods. Ellipses indicate the position estimation error standard deviations. For the identified commercial ships, their true mean positions obtained from GPS measurements, where available, are indicated by the chromatic pentagrams. Black dots represent the tow track of the coherent hydrophone array, with black triangle representing the starting location in each observation interval.

For the identified commercial ships, since their true positions are available from historical GPS records, the passive acoustic localization error using the MAT-MMSE method is quantified for these vessels, as the bias in the mean position estimate. The localization error varies between 4% to 45% with an average of roughly 16%, and depends on the bearing of the vessel from the coherent hydrophone array broadside direction, biases present in the beamformed and GPS derived bearings, as well as relative motion of the vessel and the tow ship (see Table 5).

For each passively detected ocean vessel, multiple features have been extracted from the acoustic signal detections, among which, the center frequency and bandwidth provide the most distinctive characteristics that can be employed to classify the vessel. These two features are summarized for the signal detections from the five identified commercial ships in Table 1 and the nine unidentified ocean vessels in Table 2.

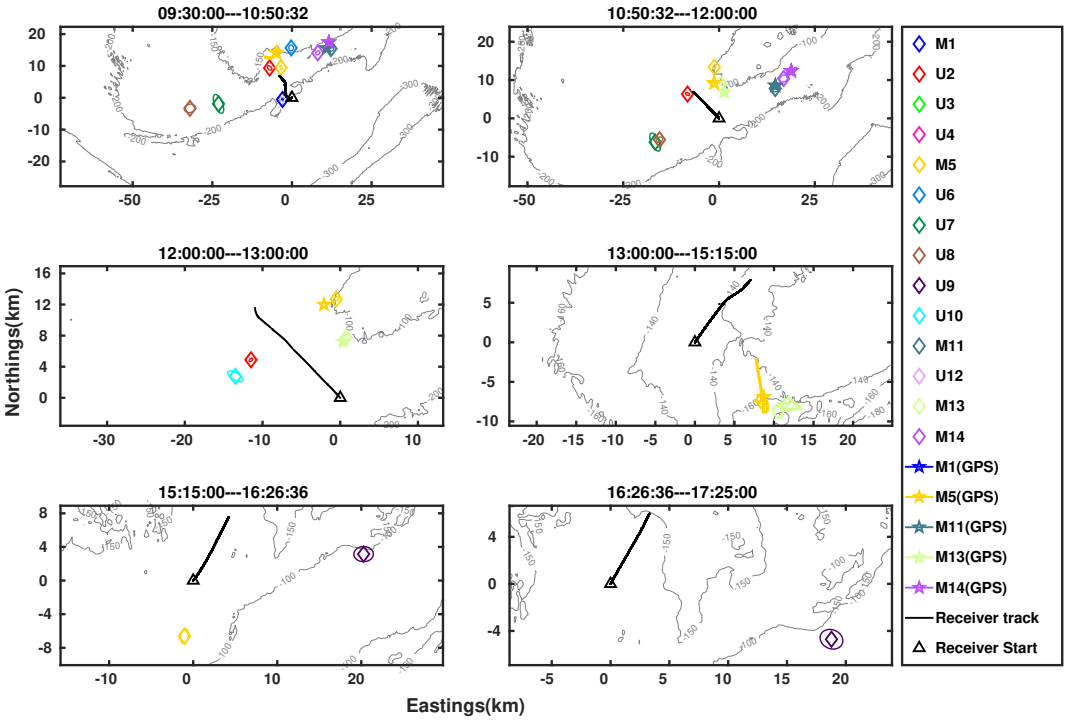

Figure 4. Similar to Figure 3, except zoomed in to around 30–50 km range of the coherent hydrophone array.

Table 1. Frequency characteristics of dominant narrowband signal detections from identified vessels on 23 February 2014 off Lofoten archipelago in the Norwegian Sea. The abbreviations used for ship types are cargo (CG) and fishing (F). The true range of the ship from the coherent hydrophone array is based on GPS measurements.

Ship Name	Center Frequency (Hz)	Bandwidth (Hz)	True Range (km)	True Speed (Knots)
WILSON	49.6	4.2 ± 1.0	39.1 ± 5.7	6.8 ± 0.6
ALGECIRAS, CG (M1)	65.6	4.4 ± 1.1	(28.6–46.0)	(5.6–7.6)
	82.6	4.6 ± 1.0		
	98.8	4.5 ± 1.2		
	339.2	6.6 ± 1.7		
	1019.5	10.7 ± 2.0		
	1357.5	10.6 ± 2.0		
	1700.7	11.2 ± 2.0		
BUEFJORD, F (M13)	49.9	4.2 ± 1.0	13.6 ± 3.2	2.0 ± 2.1
	102.0	4.1 ± 1.4		
	166.7	4.8 ± 1.7	(5.5–16.0)	(0.6–8.3)
	276.5	7.7 ± 1.4		
	553.2	6.7 ± 1.9		
	831.2	6.8 ± 1.8		
	1404.8	10.9 ± 2.0		
	1783.7	11.0 ± 1.9		
EROS, F (M14)	1081.4	10.0 ± 1.2	22.2 ± 2.7	7.5 ± 0.5
			(18.2–25.9)	(6.8–8.2)
FORTUNA, F (M11)	180.9	5.0 ± 0.4	17.7 ± 0.8	3.3 ± 1.7
	256.3	8.2 ± 2.1	(16.6–19.1)	(1.6–7.7)
	446.0	6.8 ± 1.3		
	533.4	7.9 ± 1.4		
	1198.8	10.4 ± 1.3		
FUGLOYHAV, F (M5)	74.7	3.3 ± 0.6	10.8 ± 2.4	4.6 ± 2.3
	112.7	4.0 ± 1.1	(7.1–16)	(0.2–8.4)
	421.6	7.6 ± 1.6		
	737.2	8.0 ± 2.3		
	1317.1	11.2 ± 1.9		
	1372.1	8.9 ± 2.1		
	1875.0	10.0 ± 2.2		

Table 2. Frequency characteristics of dominant narrowband signal detections from unidentified vessels on 23 February 2014 off Lofoten archipelago in the Norwegian Sea. The mean range of each unidentified vessel from the coherent hydrophone array is estimated using the the Minimum Mean Square Error implementation of Moving Array Triangulation (MAT-MMSE) technique.

Ship Name	Center Frequency (Hz)	Bandwidth (Hz)	Mean Estimated Range (km)
Unknown vessel U2	101.7	4.1 ± 0.7	5.0
	489.6	7.7 ± 2.0	
	560.5	7.4 ± 1.6	
	1123.2	9.9 ± 1.8	
	1477.6	9.3 ± 2.1	
Unknown vessel U3	167.3	5.7 ± 0.9	201.8
	238.1	8.6 ± 1.3	
Unknown vessel U4	486.5	7 ± 1.5	188.7
	1264.9	9.7 ± 1.8	
	1463.9	9.4 ± 2	
Unknown vessel U6	257.8	7.8 ± 1.9	15.6
	830.3	7.8 ± 1.7	
	1106.3	10.0 ± 2.2	
	1935.6	10.5 ± 2.1	
Unkown vessel U7	82.6	3.4 ± 0.6	19.5
Unkown vessel U8	166.8	9.7 ± 1.5	23.1
	470.3	6.9 ± 2.6	
	1049.0	8.4 ± 2.1	
Unkown vessel U9	360.7	10.0 ± 0.4	18.7
	721.4	6.8 ± 1.6	
Unkown vessel U10	167.4	9.8 ± 0.8	7.8
Unkown vessel U12	129.1	4.1 ± 1.3	173.4
	166.2	3.9 ± 1.8	

3.1.1. Commercial Ships Identified by GPS

Here we provide detailed results from our analysis for two of the five identified commercial ships, fishing vessel (FV) Fortuna (labeled M11) and FV Fugloyhav (ship now renamed to FV Vikanoy, labeled M5). The tow tracks of the coherent hydrophone array and the corresponding locations of FV Fortuna on 23 February 2014 off the Lofoten archipelago during NorEx14 based on GPS measurements are shown in Figure 5A. The bearing-time trajectories of detected signals measured by the coherent hydrophone array that are associated with FV Fortuna in the three frequency subbands, 10–200 Hz, 200–1000 Hz and 1000–2000 Hz are plotted in Figure 5B–D. The red dots represent the bearings of signal detections and the black curve are the true bearings of FV Fortuna derived from GPS-measurements. The bearings of detected signals overlap well with the true bearings in all three frequency subbands so that these acoustic signals can be associated with FV Fortuna. The time-frequency characteristics of the detected signals associated with FV Fortuna in the three frequency subbands are shown in Figure 6. The sound radiated by FV Fortuna is dominated by several distinct narrowband signals which are tonals near 180 Hz, 256 Hz, 446 Hz and 553 Hz, as well as the wavering frequency signal centered around 1200 Hz. Examples of beamformed spectrograms containing these prominent narrowband signals, as well as other broadband and narrowband signals associated with FV Fortuna are shown in Figure 6A–C. The ensemble of pitch tracks and the histogram of mean frequency weighted by signal duration [2] for the ship-associated detections in the three frequency subbands are shown in Figure 6D–I.

The horizontal track of FV FORTUNA in the time period from 10:45:05 a.m. to 11:06:50 a.m. GMT estimated from the bearing-time trajectory of its signal detections using the MAT technique is

shown in Figure 7, along with its true track based on GPS measurements. The estimated track of FV FORTUNA overlaps well with the true track, but is shorter than the true track. The mean localization error averaged over the entire track shown is roughly 5% of the true range.

Similar analysis is conducted and presented for FV Fugloyhav. The estimated bearings of signal detections that overlap with its true bearings derived from GPS measurements in all three frequency subbands are shown in Figure 8B–D. The time-frequency characteristics of the detected signals associated with FV Fugloyhav in the three frequency subbands are shown in Figure 9A–I. They include beamformed spectrogram examples containing key narrowband signals, ensemble of pitch tracks, as well as the histogram of mean frequency weighted by signal duration for the ship-associated detections.

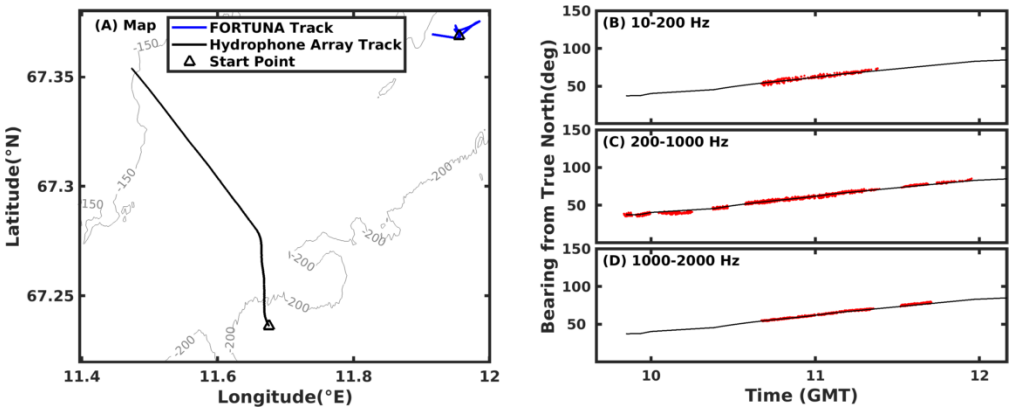

Figure 5. (**A**) locations of the FV Fortuna (labeled as vessel M11) off the Lofoten archipelago on 23 Febreuary 2014 and tow track of coherent hydrophone array during NorEx2014 over the time period shown in Figure 5(**B**–**D**). (**B**–**D**) bearing and time of signal detections (red dots) on the coherent hydrophone array that are associated with FV Fortuna (GPS derived bearing shown in black) in the three frequency subbands. There are a total of 32,352, 39,922, and 78,812 signal detections in the 10–200 Hz, 200–1000 Hz and 1000–2000 Hz frequency bands, respectively, over the 2 h observation duration analyzed here.

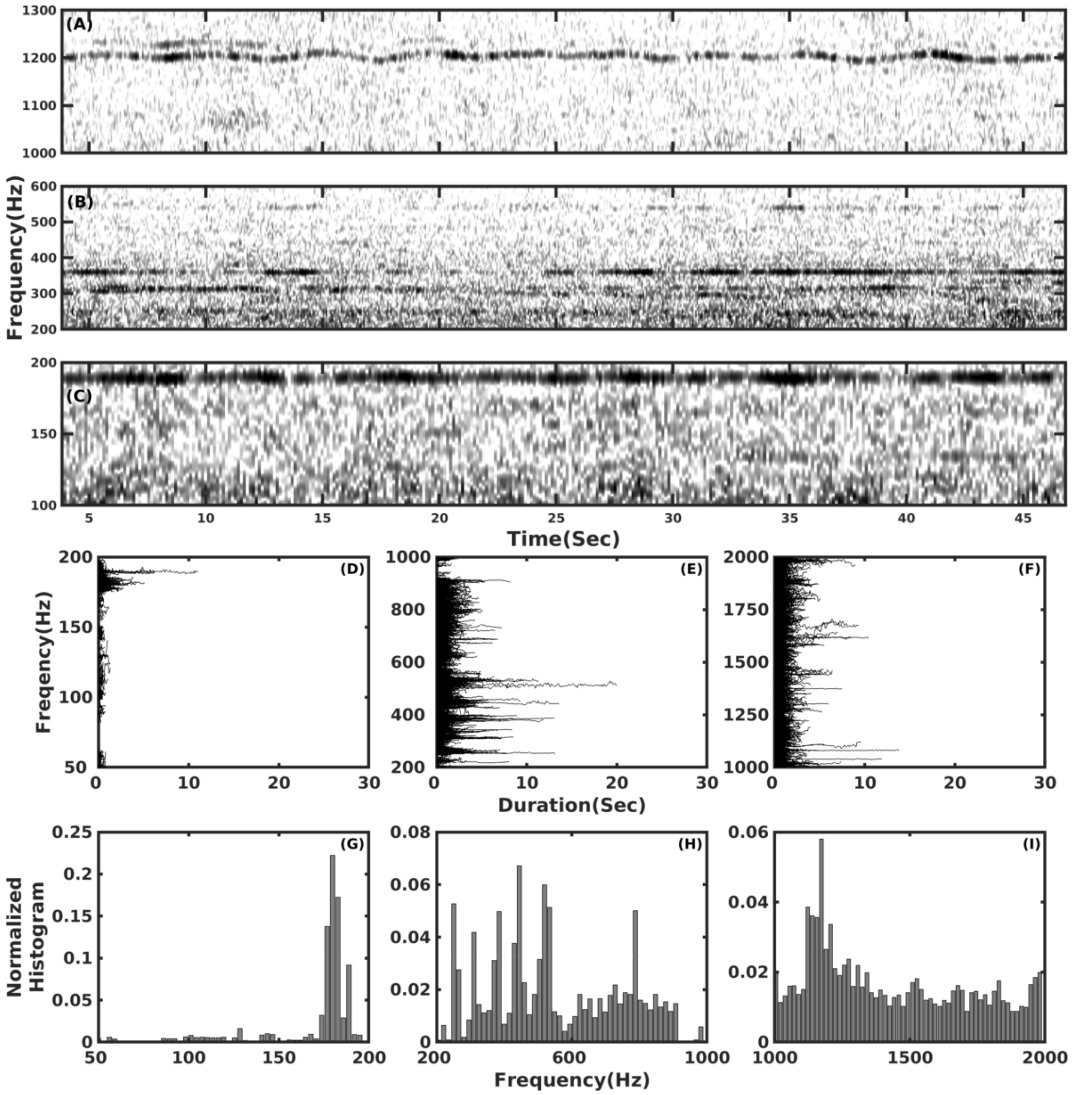

Figure 6. Characteristics of signal detections associated with Fishing Vessel (FV) Fortuna (vessel M11) during NorEx14. (**A**–**C**) examples of beamformed spectrograms containing prominent narrowband tonals and less prominent broadband signals; (**D**–**F**) pitch track ensemble for the signal detections in the 10–200 Hz, 200–1000 Hz and 1000–2000 Hz frequency ranges; (**G**–**I**) the normalized histogram of center frequency weighted by the signal duration for signal detections associated with FV Fortuna.

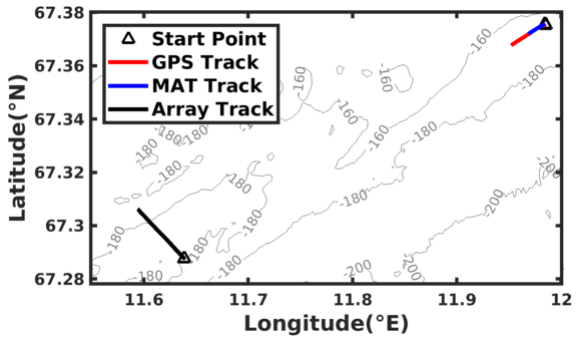

Figure 7. Passive acoustic localization of FV FORTUNA (vessel M11). The track of FV Fortuna estimated using the MAT technique from signal detections on the coherent hydrophone array in the time period from 10:45:05 a.m. to 11:06:50 a.m. GMT. The GPS measured true track of FV Fortuna is overlain for comparison.

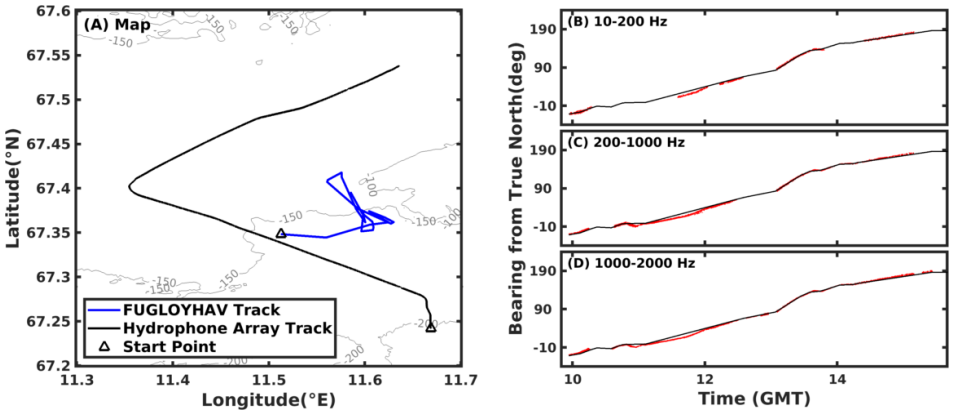

Figure 8. (**A**) locations of the FV Fugloyhav (labeled vessel M5) on 23 February 2014 off the Lofoten archipelago and tow track of coherent hydrophone array during NorEx2014 over the time period shown in Figure 8(**B**–**D**). (**B**–**D**) bearing and time of signal detections (red dots) on the coherent hydrophone array that are associated with the Fugloyhav (GPS derived bearing shown in black) in the three frequency subbands. There are a total of 77,653, 84,734, and 145,133 signal detections in the 10–200 Hz, 200–1000 Hz and 1000–2000 Hz frequency bands, respectively, over the roughly 6 h observation duration analyzed here.

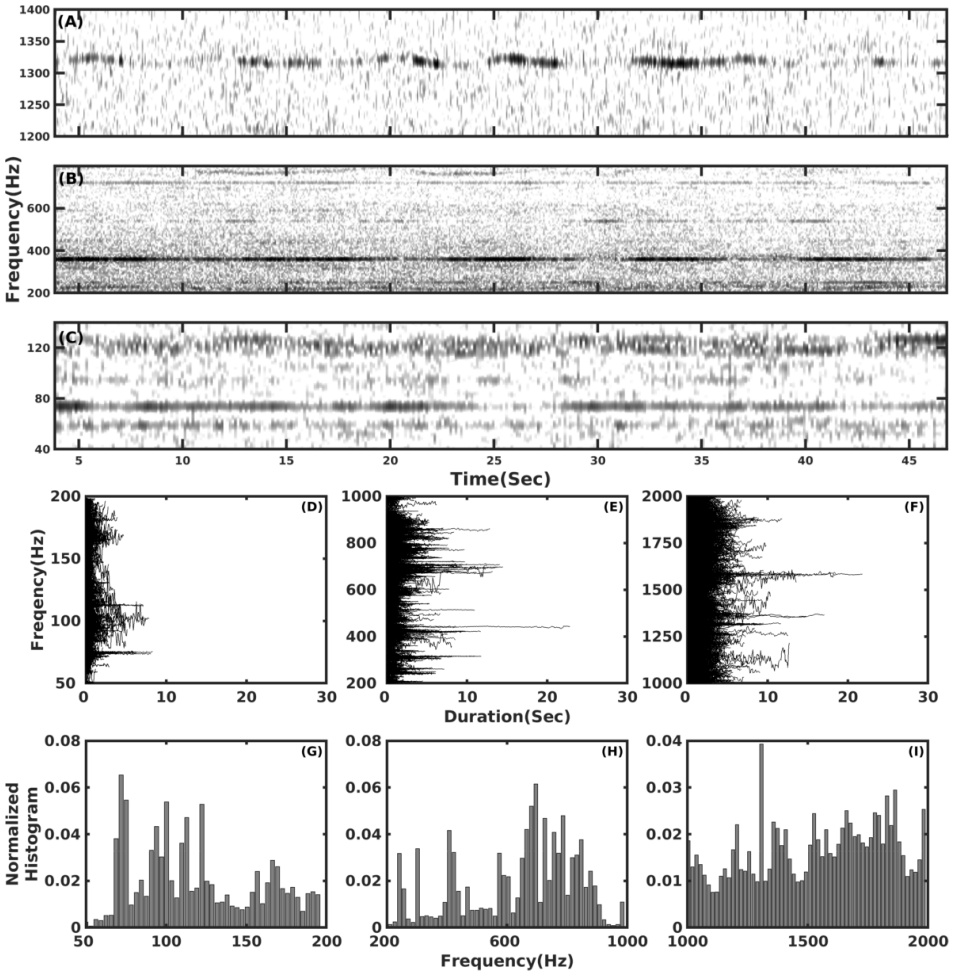

Figure 9. Characteristics of signal detections associated with FV Fugloyhav (vessel M5) during NorEx14. (**A**–**C**) examples of beamformed spectrograms containing prominent narrowband tonals and less prominent broadband signals; (**D**–**F**) pitch track ensemble for the signal detections in the 10–200 Hz, 200–1000 Hz and 1000–2000 Hz frequency ranges; (**G**–**I**) the normalized histogram of center frequency weighted by the signal duration for signal detections associated with FV Fugloyhav.

The horizontal track of FV Fugloyhav in the time period from 14:19:05 to 15:09:05 GMT estimated from the bearing-time trajectory of it signal detections using the MAT technique is shown in Figure 10, along with its true track based on GPS measurements. The estimated track of FV Fugloyhav overlaps well with the true track, but is longer than the true track in this case. The mean localization error averaged over the entire track shown is roughly 5.6% of the true range.

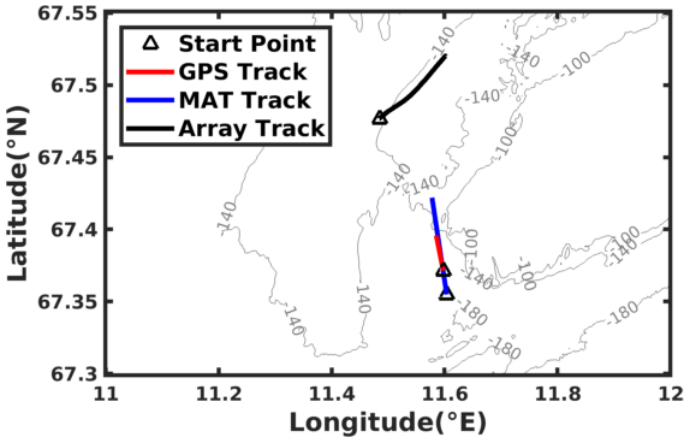

Figure 10. Passive acoustic localization of FV Fugloyhav (vessel M5). The track of FV Fugloyhav estimated using the MAT technique from signal detections on the coherent hydrophone array in the time period from 14:19:05 to 15:09:05 GMT. The GPS measured true track of FV Fugloyhav is overlain for comparison.

3.1.2. Vessels Unidentified by GPS

Nine of the 14 vessels detected by the coherent hydrophone array could not be identified based on the historical GPS record of ships accessible to us for that region. Here we provide more detailed results for two of the nine unidentified ships, which are labeled as vessels U3 and U2 in Figure 2 and Table 2, based on our analysis of the coherent hydrophone array passive acoustic data. For vessel U3, the bearing-time trajectories of signal detections and examples of beamformed spectrograms showing the detected signals are provided in Figure 11A–D. The ensemble of pitch tracks and the histogram of mean frequency weighted by signal duration for the detections associated with vessel U3 are shown in Figure 11E–H. There are only two strong narrowband tonals detected, which are centered at 167.3 Hz and 238.1 Hz. Since the mean bearing of signal detections is approximately constant over the two hour observation interval, and only tonals at very low frequencies $<$250 Hz are detected, the vessel U3 is probabaly located at very great distances from the coherent hydrophone array.

To localize vessel U3, the MAT-MMSE approach is employed to estimate its mean horizontal position and displayed in Figure 11I, including the localization error ellipse. The estimated mean horizonal position of vessel U3 is roughly 200 km away from the coherent hydrophone array. The cross range position error, determined by the bearing estimation error, is smaller than the range estimation error which is roughly 10% of the estimated range, leading to an elliptical horizontal position estimation error about the mean. The large separation $\approx$200 km between vessel U3 and the coherent hydrophone array accounts for the fact that the narrowband signals detected from it have low frequencies $<$250 Hz. The higher frequency signals radiated by this vessel have undergone significant attenuation due to absorption losses in the oceanic waveguide that is proportional to frequency, making the high frequency tonals undetectable [55–57].

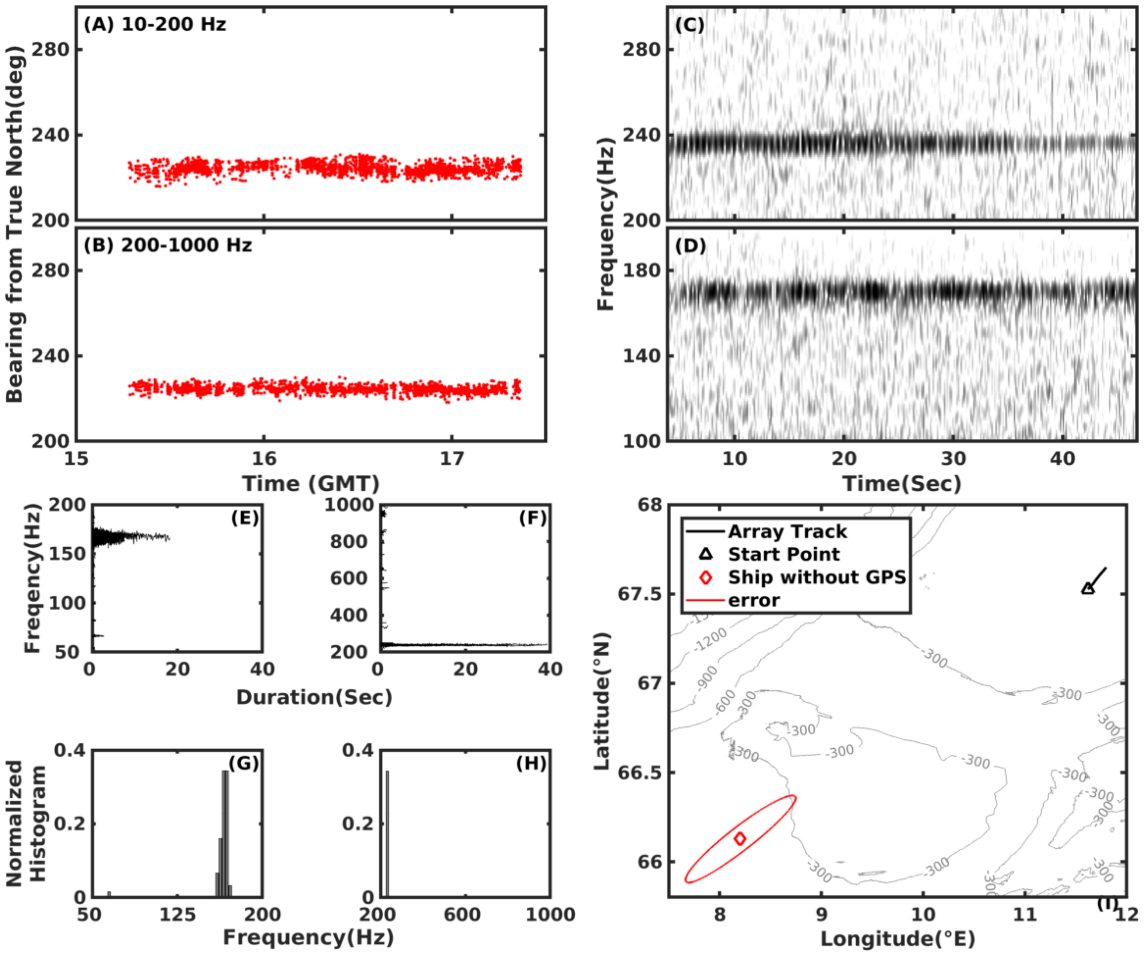

Figure 11. Signal detections, characteristics and localization associated with unidentified vessel U3 during NorEx14 on 23 February 2014 off the Lofoten archipelago. (**A**,**B**) bearing and time of signal detections (red dots) on the coherent hydrophone array that are associated with unidentified vessel U3 in the two frequency subbands shown. There are a total of 3112 and 1725 signal detections in the 10–200 Hz and 200–1000 Hz frequency bands, respectively, over the roughly 2 h observation duration analyzed here; (**C**,**D**) examples of beamformed spectrograms containing prominent narrowband tonals and less prominent broadband signals; (**E**,**F**) pitch track ensemble for signal detections in the 10–200 Hz and 200–1000 Hz frequency ranges; (**G**,**H**) the normalized histogram of center frequency weighted by signal duration for signal detections associated with unidentified vessel U3; (**I**) passive acoustic localization of vessel U3 by employing the MAT-MMSE approach.

Similar analysis conducted for another unidentified vessel U2 and displayed in Figure 12. Vessel U2 was nearby to the coherent hydrophone array since strong tonals were detected in all three frequency subbands from 10 Hz to 2000 Hz, with significant bearing variation of more than 100° over the observation time period of roughly 2.5 h. The estimated mean horizontal position of vessel U2 is shown in Figure 12M, along with its position estimation error ellipse. The vessel U2's estimated mean horizontal position is a couple to a few kilometers away from the coherent hydrophone array. This short range accounts for the detections of multiple narrowband signals in the broader frequency range from 10 Hz to 2000 Hz.

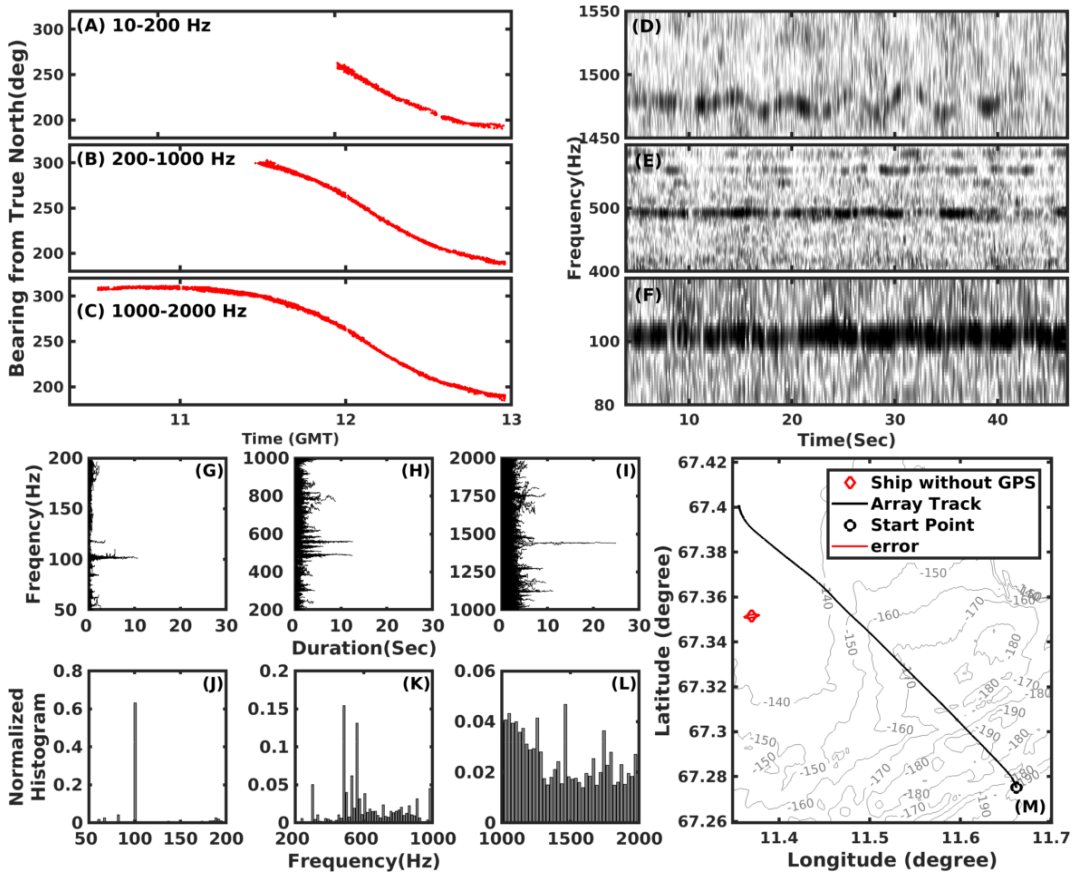

Figure 12. Signal detections, characteristics and localization associated with unidentified vessel U2 during NorEx14 on 23 February 2014 off the Lofoten archipelago. (**A**–**C**) bearing and time of signal detections (red dots) on the coherent hydrophone array that are associated with unidentified vessel U2 in the three frequency subbands shown. There are a total of 1119, 5053 and 17,390 signal detections in the 10–200 Hz, 200–1000 Hz and 1000–2000 Hz frequency bands respectively over the roughly 2.5 h observation duration analyzed here; (**D**–**F**) examples of beamformed spectrograms containing prominent narrowband tonals and less prominent broadband signals; (**G**–**I**) pitch track ensemble for signal detections in the 10–200 Hz, 200–1000 Hz and 1000–2000 Hz frequency ranges; (**J**–**L**) the normalized histogram of center frequency weighted by signal duration for signal detections associated with unidentified vessel U2; (**M**) passive acoustic localization of vessel U2 by employing the MAT-MMSE approach.

3.2. Simultaneous Passive Acoustic Detection and Localization of Multiple Ocean Vessels on 26 February off Northern Finnmark

Here we provide a summary of the ocean vessels detected by the coherent hydrophone array on 26 February 2014 off the Northern Finnmark region. The bearing and time of all detected acoustic signals in the 10 Hz to 2000 Hz frequency range that stand at least 5.6 dB above the local ambient background noise in the beamformed spectrograms are displayed as grey dots in Figure 13A–C. In each of the three frequency subbands, there are once again more than 100,000 signal detections in the roughly 7.5 h observation time interval shown. In addition to sounds radiated by mechanized ocean vessels, the signal detections include marine mammal vocalizations [1], sounds from fish and other ocean biology, as well as other either made-made or natural acoustic and seismic sources. The signal detections from the 16 vessels, shown in color, follow distinct and well-defined bearing-time trajectories. Of the 16 vessels detected using passive acoustics, 15 are identified as commercial ships by comparison with historical GPS information of ships in that region and coincident time period. Their labels and identities are provided in Table 3. The remaining single unidentified vessel is labeled as U16 in Figure 13C and Table 4. The MAT-MMSE approach is employed to localize the single unidentified

vessel and shown in Figure 14. The GPS measured tracks are shown for the identified commercial ship and the tow ship in Figure 14.

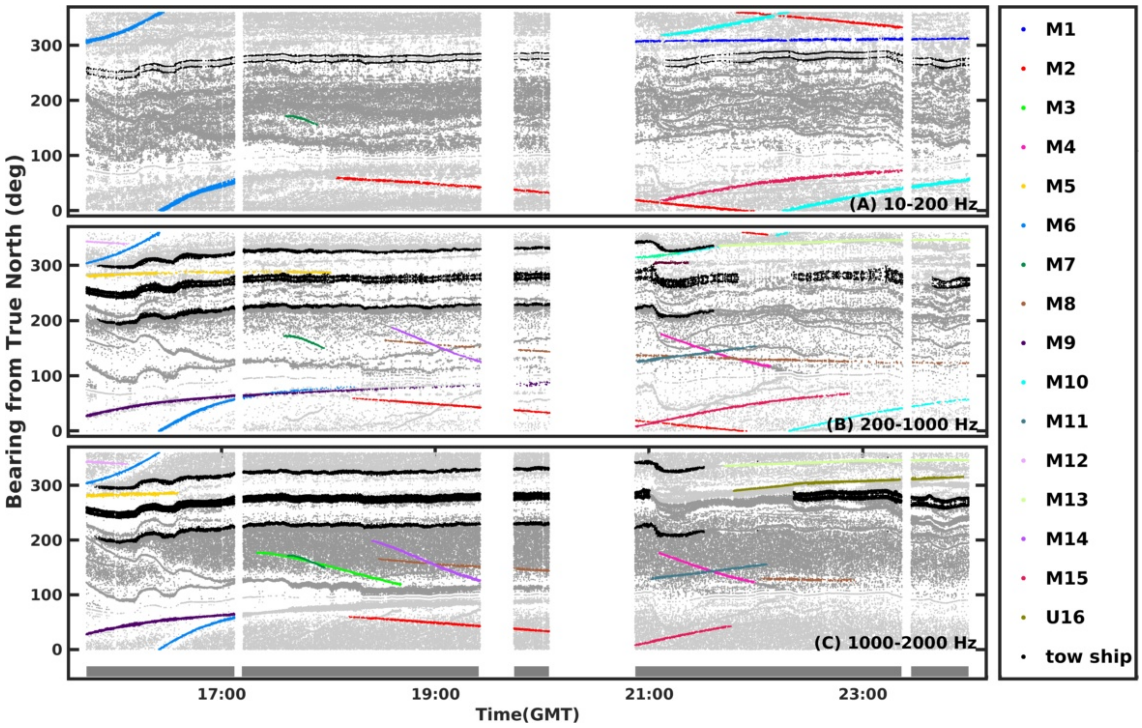

Figure 13. Extracting signal detections from multiple mechanized ocean vessels on 26 February 2014 off Northern Finnmark in the (**A**) 10–200 Hz; (**B**) 200–1000 Hz; and (**C**) 1000–2000 Hz frequency subbands. The bearing and time of all detected signals are indicated in gray, spanning a 360-degree horizontal azimuth about the coherent hydrophone array from true north. Light and dark gray dots correspond to right and left side bearings respectively for all detections about the receiver array, before the line array's left-right bearing ambiguity resolution [8]. Chromatic dots represent signals generated by multiple vessels. The vessels with labels M1 to M15 have been identified as commercial ships (refer to Table 3 for ship name), while the vessel with label U16 has not been identified. The black dots correspond to signals radiated by the tow ship (see Appendix A). The light gray bar at the bottom shows the coherent hydrophone array recording time intervals.

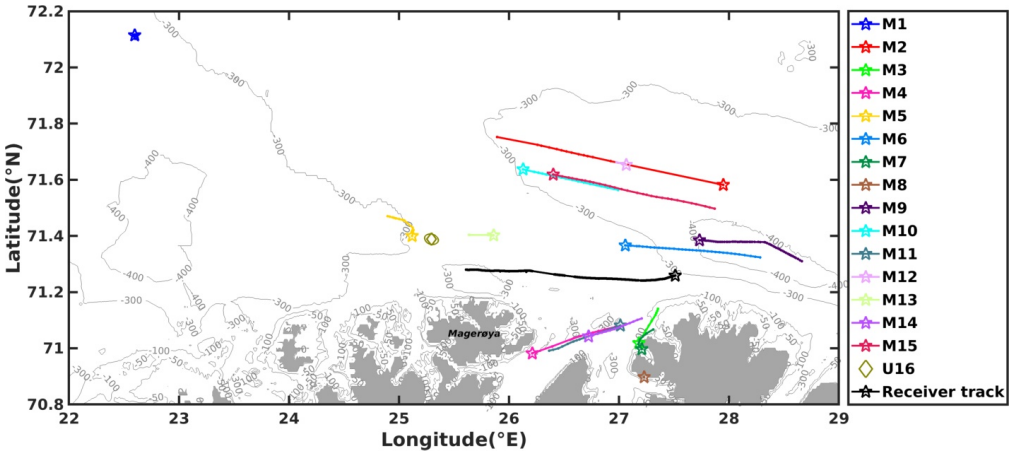

Figure 14. Geographic positions of passively detected mechanized ocean vessels on 26 February 2014 off northern Finnmark. The mean position (diamond) of the unidentified vessel U16 is estimated using the MAT-MMSE technique. The GPS measured positions are shown for the remaining identified commercial ships with pentagrams indicating their starting locations.

Table 3. Frequency characteristics of dominant narrowband signal detections from identified vessels on 26 February 2014 off Northern Finnmark in the Norwegian Sea. The abbreviations used for ship types are cargo (CG), fishing (F), reefer cargo (RCG), passenger (P), search and rescue (SAR) and tanker (T). The true range of the ship from the coherent hydrophone array is based on GPS measurements.

Ship Name	Center Frequency (Hz)	Bandwidth (Hz)	True Range (km)	True Speed (knots)
Esvagt Castor, SAR (M1)	170.9	4.4 ± 1.0	148.5 ± 5.4 (140.3–185.1)	1.2 ± 2.1 (0.2–6.6)
Federal Rhine, CG (M2)	95.5 290.4 1121.2 1533.6 1609.7	4.7 ± 1.6 10.6 ± 1.5 10.7 ± 2 10.3 ± 2.1 10.1 ± 2.2	50.6 ± 2.8 (48.8–57.2)	13.3 ± 0.3 (12.7–13.7)
Henriksen Jr, F (M3)	1523.9 1590.3	8.6 ± 1.3 5.7 ± 0.9	23.5 ± 1.7 (21.6–26.3)	6.6 ± 0.7 (5.4–7.5)
Holmfoss, RCG (M4)	609.2 894.7 1791.1	7.2 ± 1.6 9.4 ± 1.7 11.0 ± 1.7	36.6 ± 4.4 (31.8–44.4)	15.4 ± 0.2 (15–15.7)
Kapitan Durachenko, F (M5)	840.9 1041.6 1147.0 1469.7	8 ± 1.2 9.7 ± 1.9 10.8 ± 1.6 9.4 ± 1.2	82.8 ± 1.3 (81.9–86.5)	3.9 ± 0.2 (3.6–4.2)
Kepromar, F (M6)	49.4 73.9 312.7 1011.7 1990.1	5.4 ± 0.5 5 ± 0.7 8.9 ± 1.6 10.9 ± 1.6 11.0 ± 2.1	25.1 ± 12.0 (12.5–51.6)	9.9 ± 0.5 (9.2–10.7)
Nordlys, P (M7)	492.7 737.9 767.2 1545.3 1600.9	9.3 ± 1.2 10.2 ± 1.5 9.6 ± 1.3 10.0 ± 2.7 9.6 ± 2.8	24.7 ± 1.9 (23.1–27.9)	14.4 ± 0.3 (14.1–14.9)
Nordstrand, F (M8)	765.6 893.4	11.3 ± 2.2 10.8 ± 2.5	61.0 ± 8.4 (43.5–72.1)	0.3 ± 0.2 (0–0.7)
Persey-4, F (M9)	652.4 988.2 1458.6	9.4 ± 1.8 10.6 ± 1.3 9.8 ± 1.7	46.3 ± 19.5 (16.3–80.3)	4.5 ± 0.5 (3–5.9)
RN Murmansk, T (M10)	66.1 420.4	4.7 ± 0.4 9 ± 1.8	48.2 ± 5.5 (41.7–58.6)	12.9 ± 0.3 (12.2–13.4)
Troma, T (M11)	510.7 560.7 764.3 1008.3 1757.6	7.7 ± 1.4 7.3 ± 1.7 10.0 ± 2.0 10.2 ± 1.7 9.8 ± 1.8	34.9 ± 0.6 (34.2–36.1)	11.8 ± 0.4 (10.8–12.3)
United Fortune, CG (M12)	394.9 438.7 1152.6	11.3 ± 1.1 9.9 ± 1.1 11.2 ± 1.7	47.6 ± 2.0 (44.9–50.0)	11.7 ± 0.2 (11.6–12.0)
Variant, F (M13)	459.0 541.0 824.3 1531.2	9.8 ± 1.42 9.5 ± 1.2 10.3 ± 1.5 11.5 ± 1.8	15.0 ± 0.6 (14.3–15.5)	3.0 ± 0.3 (2.4–3.3)
Wilson Husum, CG (M14)	538.6 950.8 1023.6 1123.1	8.7 ± 1.6 8.7 ± 1.5 9.6 ± 1.8 10.4 ± 1.1	23.4 ± 1.9 (21.6–27.5)	11.4 ± 0.3 (11–11.9)
Wolgastern, T (M15)	118.6 561.7 1106.7	5.3 ± 0.8 9.2 ± 1.4 10.6 ± 1.8	150.0 ± 10.1 (38.9–70.0)	11.9 ± 0.5 (11–12.9)

For each passively detected ocean vessel, the center frequency and bandwidth of the most prominent narrowband signals are provided in Tables 3 and 4 for the identified commercial ships and the single unidentified vessel, respectively.

Table 4. Frequency characteristics of dominant narrowband signal detections from the unidentified vessel on 26 February 2014 off Northern Finnmark in the Norwegian Sea. The mean range of the unidentified vessel from the coherent hydrophone array is estimated using the MAT-MMSE technique.

Ship Name	Center Frequency (Hz)	Bandwidth (Hz)	Estimated Range (km)
Unknown vessel (U16)	1043.6	10.2 ± 1.8	21.6

Table 5. Normalized bias in mean source position estimate from passive acoustic localization of the identified commercial ships on 23 February 2014 off the Lofoten archipelago using the MAT-MMSE method. The mean localization error averaged over the results for all ships is roughly 16% of the true range.

Ship Name	09:30:00–10:50:32	10:50:32–12:00:00	12:00:00–13:00:00	13:00:00–15:15:00
WILSON ALGECIRAS (M1)		9.53%		
FUGLOYHAV (M5)	32.43%	44.49%	14.17%	5.27%
FORTUNA (M11)	7.16%	4.62%		
BUEFJORD (M13)		32.18%	9.06%	8.13%
EROS (M14)	22.93%	12.40%		

4. Discussion

Over the roughly 8 h observation interval per day for the two days analyzed here, a total of 30 mechanized ocean vessels have been identified and characterized based on acoustic recordings of its underwater radiated sound received by a coherent hydrophone array. Twenty of these vessels can be confidently identified since the bearing-time trajectories of the signal detections from these vessels and passively localized horizontal positions match well with coincident measured bearings and locations derived from historical GPS information. The GPS information from these ships is sufficiently dense to provide multiple points of bearing and location correspondence with those based on acoustic detections. The remaining 10 vessels could not be identified or confidently associated with historical GPS information. For instance, the unknown vessel U2 acoustically detected on 23 February 2014 off the Lofoten Archipelago could have been the Norwegian trawler Langoey. This is because the estimated position of vessel U2 corresponds well with the GPS measured location of trawler Langoey. However, the historical GPS position information available to us for the trawler Langoey is sparse in the time period from 09:50:00 to 13:00:00 GMT where we have significant acoustic detections. Only one measured GPS position is available in this time period and so has only one-point correspondence between the GPS derived and acoustic detection bearings. Similarly, the unknown vessel U12 could be the well stimulation vessel, Island Wellserver, again based on one point correspondence with GPS derived bearing and location as only one GPS measurement is present in the historical records during the acoustic detection time period. The vessel U12 could also be the vessel U3 because both these acoustic detections emanate at long ranges $>$200 km from the coherent hydrophone array and the localized positions match well (see Figure 3). Furthermore, both these acoustic detection tracks include a low frequency tonal centered at 166-167 Hz. However, since they were detected at non-overlapping time intervals, and each has one other narrowband signal that doesn't coincide in frequency, we assigned separate vessel labels to these acoustic detections. There are potential associations for a few of the other unidentified vessels based on bearing and localization result, but the acoustic detections and the GPS information are in mutually exclusive time periods. These potential associations include cargo ship Zapolyarye for unidentified vessel U4 and fishing vessel Almak for unidentified vessel U7 off the Lofoten archipelago.

The time-frequency characteristics of the narrowband signals radiated from each of the ocean vessels examined here and tabulated in Tables 1–4 are based on analysis time periods of at least 30 min to over 4 h. Each ocean vessel radiates multiple dominant narrowband signals, with unique set of frequencies that can be employed to distinguish and classify the vessel [28]. The time-frequency characteristics of the narrowband signals from the identified commercial ships and the unidentified vessels provided here can be employed for future real-time automated passive acoustic classification of these vessels. A variety of automated classification techniques [53] such as logistic regression, decision tree [58] and support vector machine (SVM) can employ the time-frequency characteristics of the ship radiated sound directly for classification. Other approaches, such as neural networks [53,59–61], can be trained using the beamformed time series or spectrogram images containing the ship radiated signals as inputs for direct classification.

In [2], the speed and direction of a distant ship was found to change the relative level of importance of the narrowband signals, but did not significantly alter the frequencies of these signals. Doppler effects may become important for ocean vessel moving in close proximity to a receiver. Vessel activity, such as offshore piling, seismic profiling and fish trawling can lead to additional complexity in the sound field, can be accounted for after long term monitoring. The analysis of sound radiated from multiple ships presented here is expected to influence ship design [2,33,62] and methods for reducing overall ship-radiated noise level and impact on biological organisms, as well as approaches for monitoring ships in ocean surveillance and shipping traffic regulation.

5. Conclusions

Multiple mechanized ocean vessels have been simultaneously monitored from their underwater radiated sounds received on a large-aperture densely-sampled coherent hydrophone array over continental-shelf scale regions $>$10,000 km^2 in the Norwegian Sea. Coherent beamforming of the acoustic data received on the coherent hydrophone array enables directional sensing in a 360-degree horizontal azimuth about the receiver array. Furthermore, coherent processing also increases the SNR which enhances ship detection ranges by roughly two orders of magnitude over that of a single hydrophone. A total of approximately 30 mechanized ocean vessels have been detected, classified and localized from their underwater sounds present in acoustic recordings of over 8 h per day for two days. These vessels are detected at varying ranges from the coherent hydrophone array spanning nearby to over 150 km. The underwater sound received from the mechanized ocean vessels are dominated by narrowband signals that are either constant frequency tonals or have frequencies that waver or oscillate slightly in time. The mean horizontal positions of these vessels from the receiver array center are estimated using the MAT technique from sequences of corresponding bearing measurements. Twenty of these vessels are identified as commercial ships whose bearing-time trajectories and estimated positions derived from underwater signal detections have been verified with GPS information recorded in historical AIS database for the region with multiple points of correspondence with the acoustic measurements. The remaining approximately ten vessels remain unidentified because of sparse or absent GPS information during our recording time interval. Analysis of identified commercial ship acoustic data indicates the MAT method for passive localization of surface ships leads to localization errors of roughly 5–30% of the true range, depending on the bearing of the vessel from the coherent hydrophone array broadside direction, as well as biases in beamformed and GPS derived bearings.

Author Contributions: Data analysis and interpretation was conducted primarily by C.Z., with contributions from H.G., A.K., M.S., N.O.H., O.R.G., W.H. and P.R.; C.Z. and P.R. wrote the paper; research was directed by P.R.

Funding: This research was funded by United States Office of Naval Research grant number N00014-17-1-2476 and the United States National Science Foundation grant number OCE-1736749.

Acknowledgments: This research was also supported by the Norwegian Institute of Marine Research—Bergen.

Conflicts of Interest: The authors declare no conflict of interest.

Appendix A. Time-Frequency Characteristics of Dominant Narrowband Signal Detections from the Tow Ship, RV Knorr

The sound radiated by the tow ship, RV Knorr, was consistently detected in the forward endfire direction and roughly 45-degree angle from the forward direction (see Figures 2, 13 and Table A1). The detections in the forward direction correspond to the direct arrival of signals radiated by RV Knorr at the coherent hydrophone array. The detections at roughly 45 degrees angle from the forward direction correspond to signals that have undergone single bottom-bounce reflections in the approximately 150–200 m deep water column before arriving at the hydrophone array located approximately 280–330 m behind the tow ship.

The signal detected in the forward direction is dominated by several distinct narrowband tonals and wavering frequency components in all three frequency subbands, 10–200 Hz, 200–1000 Hz and 1000–2000 Hz. Examples of beamformed spectrograms containing these narrowband signals, as well as other broadband signal detections associated with the tow ship in the forward endfire direction are shown in Figure A1A–E. The ensemble of pitch tracks and the histogram of mean frequency weighted by signal duration for the ship-associated detections in the three frequency subbands are shown in Figure A1F–K.

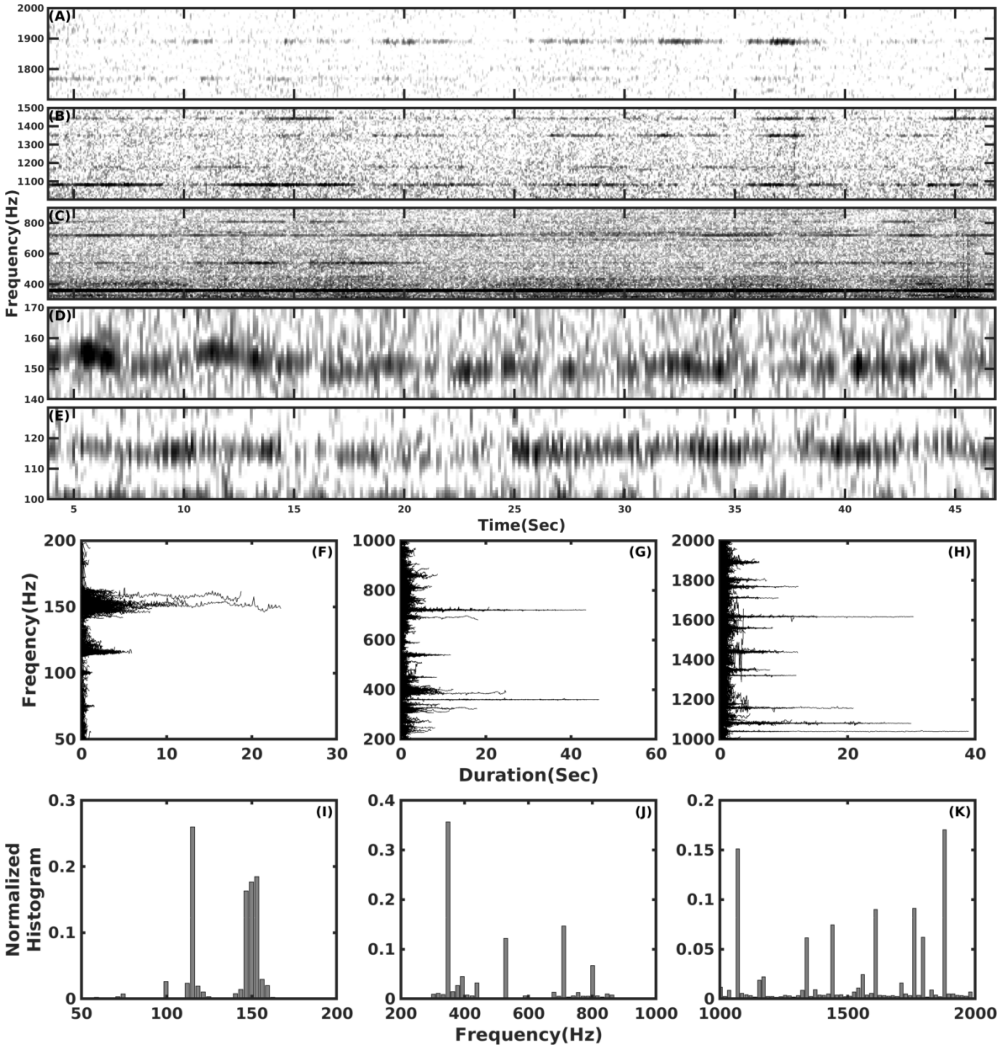

Figure A1. Characteristics of signal detections associated with tow ship, Research Vessel (RV) Knorr, in the forward endfire direction during NorEx14. (**A**–**E**) examples of beamformed spectrograms containing prominent narrowband tonals and less prominent broadband signals; (**F**–**H**) pitch track ensemble for signal detections in the 10–200 Hz, 200–1000 Hz and 1000–2000 Hz frequency ranges; (**I**–**K**) the normalized histogram of center frequency weighted by signal duration for signal detections.

The signals arriving at a roughly 45-degree angle of the forward direction is also dominated by several distinct narrowband tonals, but in only two frequency subbands, 200–1000 Hz and 1000–2000 Hz. Examples of beamformed spectrograms containing these narrowband signals, as well as other broadband detections associated with the tow ship in this angle are shown in Figure A2A,B. The ensemble of pitch tracks and the histogram of mean frequency weighted by signal duration for the ship-associated detections in the two frequency subbands are shown in Figure A2C–F.

The signals from the tow ship received by the coherent hydrophone array in the two main directions, forward endfire and roughly 45 degrees from the forward, contain many narrowband tonals at identical or nearly identical frequencies, which are in Hertz at approximately 360, 450, 540, 721, 810, 1082, 1350, 1442, 1768, 1803, 1891. The frequency characteristics of those signals are shown in Table A1.

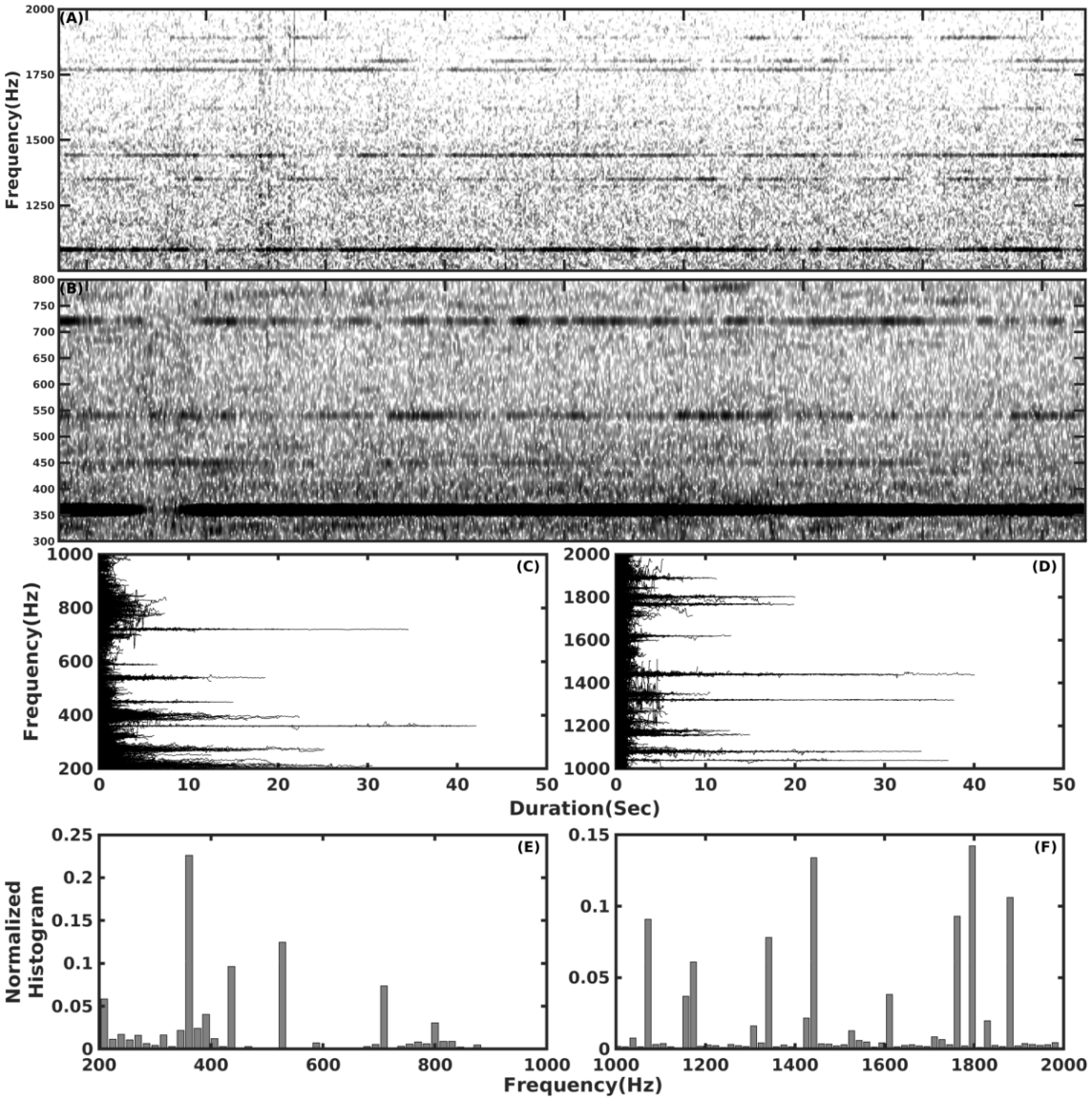

Figure A2. Characteristics of signal detections associated with tow ship, RV Knorr, at approximately 45° from the forward endfire direction during NorEx14. (**A**,**B**) examples of beamformed spectrograms containing prominent narrowband tonals and less prominent broadband signals; (**C**,**D**) pitch track ensemble of signal detections in the 200–1000 Hz and 1000–2000 Hz frequency ranges; (**E**,**F**) the normalized histogram of center frequency weighted by signal duration for signal detections.

Table A1. Frequency characteristics of dominant narrowband signal detections from tow ship, RV Knorr, in the forward endfire direction and roughly 45° from the forward direction received by the coherent hydrophone array.

Forward Endfire		45° from Forward Endfire	
Center Frequency (Hz)	**Bandwidth (Hz)**	**Center Frequency (Hz)**	**Bandwidth (Hz)**
115.9	5.3 ± 0.6	214.6	8.5 ± 1.4
360.6	9.9 ± 0.5	360.5	10.0 ± 0.3
151.0	4.5 ± 1.3	450.3	5.6 ± 1.1
450.4	6.5 ± 2.0	540.3	7.2 ± 1.7
540.1	7.8 ± 2.1	721.1	6.6 ± 1.2
721.2	8.7 ± 1.4	809.9	6.0 ± 1.4
810.1	7.8 ± 1.9	1081.6	9.8 ± 1.5
1081.8	9.8 ± 1.1	1178.8	10.4 ± 2.1
1350.6	10.2 ± 1.4	1350.5	10.0 ± 2.2
1442.3	9.7 ± 1.2	1442.1	9.6 ± 1.1
1619.8	10.4 ± 1.6	1768.6	9.8 ± 1.7
1768.5	10.4 ± 1.1	1803.1	9.4 ± 1.0
1803.0	10.1 ± 1.4	1890.8	9.6 ± 1.3
1891.0	10.3 ± 1.2		

References

1. Garcia, H.A.; Zhu, C.; Schinault, M.E.; Kaplan, A.I.; Handegard, N.O.; Godø, O.R.; Ahonen, H.; Makris, N.C.; Wang, D.; Huang, W.; et al. Temporal–spatial, spectral, and source level distributions of fin whale vocalizations in the Norwegian Sea observed with a coherent hydrophone array. *ICES J. Mar. Sci.* **2018**, fsy127. [CrossRef]
2. Huang, W.; Wang, D.; Garcia, H.; Godø, O.R.; Ratilal, P. Continental Shelf-Scale Passive Acoustic Detection and Characterization of Diesel-Electric Ships Using a Coherent Hydrophone Array. *Remote Sens.* **2017**, *9*, 772. [CrossRef]
3. Wang, D.; Garcia, H.; Huang, W.; Tran, D.D.; Jain, A.D.; Yi, D.H.; Gong, Z.; Jech, J.M.; Godø, O.R.; Makris, N.C.; et al. Vast assembly of vocal marine mammals from diverse species on fish spawning ground. *Nature* **2016**, *531*, 366. [CrossRef] [PubMed]
4. Wang, D.; Huang, W.; Garcia, H.; Ratilal, P. Vocalization source level distributions and pulse compression gains of diverse baleen whale species in the Gulf of Maine. *Remote Sens.* **2016**, *8*, 881. [CrossRef]
5. Huang, W.; Wang, D.; Ratilal, P. Diel and Spatial Dependence of Humpback Song and Non-Song Vocalizations in Fish Spawning Ground. *Remote Sens.* **2016**, *8*, 712. [CrossRef]
6. Gong, Z.; Jain, A.D.; Tran, D.; Yi, D.H.; Wu, F.; Zorn, A.; Ratilal, P.; Makris, N.C. Ecosystem scale acoustic sensing reveals humpback whale behavior synchronous with herring spawning processes and re-evaluation finds no effect of sonar on humpback song occurrence in the Gulf of Maine in Fall 2006. *PLoS ONE* **2014**, *9*, e104733. [CrossRef] [PubMed]
7. Tran, D.D.; Huang, W.; Bohn, A.C.; Wang, D.; Gong, Z.; Makris, N.C.; Ratilal, P. Using a coherent hydrophone array for observing sperm whale range, classification, and shallow-water dive profiles. *J. Acoust. Soc. Am.* **2014**, *135*, 3352–3363. [CrossRef] [PubMed]
8. Gong, Z.; Tran, D.D.; Ratilal, P. Comparing passive source localization and tracking approaches with a towed horizontal receiver array in an ocean waveguide. *J. Acoust. Soc. Am.* **2013**, *134*, 3705–3720. [CrossRef] [PubMed]
9. Hildebrand, J.A. Anthropogenic and natural sources of ambient noise in the ocean. *Mar. Ecol. Prog. Ser.* **2009**, *395*, 5–20. [CrossRef]
10. Stojanovic, M. Underwater acoustic communications. In Proceedings of the Electro/95 International, Boston, MA, USA, 21–23 June 1995; pp. 435–440.
11. Stojanovic, M.; Preisig, J. Underwater acoustic communication channels: Propagation models and statistical characterization. *IEEE Commun. Mag.* **2009**, *47*, 84–89. [CrossRef]
12. Dambra, R.; Firenze, E. Underwater Radiated Noise of a Small Vessel. In Proceedings of the 22nd International Congress on Sound and Vibration, Florence, Italy, 12–16 July 2015; pp. 12–16.

13. Merchant, N.D.; Witt, M.J.; Blondel, P.; Godley, B.J.; Smith, G.H. Assessing sound exposure from shipping in coastal waters using a single hydrophone and Automatic Identification System (AIS) data. *Mari. Pollut. Bull.* **2012**, *64*, 1320–1329. [CrossRef] [PubMed]
14. Vasconcelos, R.O.; Amorim, M.C.P.; Ladich, F. Effects of ship noise on the detectability of communication signals in the Lusitanian toadfish. *J. Exp. Biol.* **2007**, *210*, 2104–2112. [CrossRef] [PubMed]
15. Codarin, A.; Wysocki, L.E.; Ladich, F.; Picciulin, M. Effects of ambient and boat noise on hearing and communication in three fish species living in a marine protected area (Miramare, Italy). *Mari. Pollut. Bull.* **2009**, *58*, 1880–1887. [CrossRef] [PubMed]
16. Ona, E.; Godø, O.R.; Handegard, N.O.; Hjellvik, V.; Patel, R.; Pedersen, G. Silent research vessels are not quiet. *J. Acoust. Soc. Am.* **2007**, *121*, EL145–EL150. [CrossRef] [PubMed]
17. Mitson, R. Underwater noise radiated by research vessels. *ICES Mar. Sci. Symp.* **1993**, *196*, 147–152.
18. Mitson, R.B.; Knudsen, H.P. Causes and effects of underwater noise on fish abundance estimation. *Aquat. Living Resour.* **2003**, *16*, 255–263. [CrossRef]
19. Hatch, L.; Clark, C.; Merrick, R.; Van Parijs, S.; Ponirakis, D.; Schwehr, K.; Thompson, M.; Wiley, D. Characterizing the relative contributions of large vessels to total ocean noise fields: A Case study using the Gerry E. Studds Stellwagen Bank National Marine Sanctuary. *Environ. Manag.* **2008**, *42*, 735–752. [CrossRef] [PubMed]
20. Veirs, S.; Veirs, V.; Wood, J.D. Ship noise extends to frequencies used for echolocation by endangered killer whales. *PeerJ* **2016**, *4*, e1657. [CrossRef] [PubMed]
21. Wittekind, D.K. A simple model for the underwater noise source level of ships. *J. Ship Prod. Des.* **2014**, *30*, 7–14. [CrossRef]
22. Erbe, C.; McCauley, R.; Gavrilov, A. Characterizing marine soundscapes. In *The Effects of Noise on Aquatic Life II*; Springer: New York, NY, USA, 2016; pp. 265–271.
23. Miksis-Olds, J.L.; Martin, B.; Tyack, P.L. Exploring the Ocean Through Soundscapes. *Acoust. Today* **2018**, *14*, 26–34.
24. Porter, M.; Henderson, L. Global ocean soundscapes. In Proceedings of the Meetings on Acoustics ICA2013, Montreal, QC, Canada, 2–7 June 2013; Volume 19, p. 010050.
25. Crocker, S.E.; Nielsen, P.L.; Miller, J.H.; Siderius, M. Geoacoustic inversion of ship radiated noise in shallow water using data from a single hydrophone. *J. Acoust. Soc. Am.* **2014**, *136*, EL362–EL368. [CrossRef] [PubMed]
26. Hallett, M.A. Characteristics of merchant ship acoustic signatures during port entry/exit. In Proceedings of the Annual Conference of the Australian Acoustical Society, Gold Coast, Australia, 3–5 November 2004.
27. Bruno, M.; Chung, K.W.; Salloum, H.; Sedunov, A.; Sedunov, N.; Sutin, A.; Graber, H.; Mallas, P. Concurrent use of satellite imaging and passive acoustics for maritime domain awareness. In Proceedings of the 2010 International Waterside Security Conference (WSS), Carrara, Italy, 3–5 November 2010; pp. 1–8.
28. Chung, K.W.; Sutin, A.; Sedunov, A.; Bruno, M. DEMON acoustic ship signature measurements in an urban harbor. *Adv. Acoust. Vib.* **2011**, *2011*, 952798. [CrossRef]
29. Sutin, A.; Bunin, B.; Sedunov, A.; Sedunov, N.; Fillinger, L.; Tsionskiy, M.; Bruno, M. Stevens passive acoustic system for underwater surveillance. In Proceedings of the 2010 International Waterside Security Conference (WSS), Carrara, Italy, 3–5 November 2010; pp. 1–6.
30. Nejedl, V.; Stoltenberg, A.; Schulz, J. Free-field measurements of the radiated and structure borne sound of RV "Planet". In Proceedings of the Meetings on Acoustics ECUA2012, Edinburgh, UK, 2–6 July 2012; Volume 17, p. 070061.
31. McKenna, M.F.; Ross, D.; Wiggins, S.M.; Hildebrand, J.A. Underwater radiated noise from modern commercial ships. *J. Acoust. Soc. Am.* **2012**, *131*, 92–103. [CrossRef] [PubMed]
32. Urick, R.J. *Principles of Underwater Sound*; Peninsula Publishing: Los Altos Hills, CA, USA, 1983.
33. Mitson, R. *Underwater Noise of Research Vessels*; ICES Co-Operative Research Report; ICES: Oxford, UK, 1995; Volume 61.
34. Fréchou, D.; Dugué, C.; Briançon-Marjollet, L.; Fournier, P.; Darquier, M.; Descotte, L.; Merle, L. Marine Propulsor Noise Investigations in the Hydroacoustic Water Tunnel "GTH". In *Twenty-Third Symposium on Naval Hydrodynamics*; Office of Naval Research Bassin d'Essais des CarenesNational Research Council: Alexandria, VA, USA, 2001.

35. Bush, V.; Conant, J.B.; Tate, J.T. *Principles and Applications of Underwater Sound*; Technical Report; Office of Scientific Research and Development: Washington, DC, USA, 1946; Volume 7.
36. Norwood, C. An introduction to ship radiated noise. *Acoust. Aust.* **2002**, *30*, 21–25.
37. Ojak, W. Vibrations and waterborne noise on fishery vessels. *J. Ship Res.* **1988**, *32*, 22.
38. Gray, L.M.; Greeley, D.S. Source level model for propeller blade rate radiation for the world's merchant fleet. *J. Acoust. Soc. Am.* **1980**, *67*, 516–522. [CrossRef]
39. Grelowska, G.; Kozaczka, E.; Kozaczka, S.; Szymczak, W. Underwater noise generated by a small ship in the shallow sea. *Arch. Acoust.* **2013**, *38*, 351–356. [CrossRef]
40. Becker, K.; Preston, J. The ONR five octave research array (FORA) at Penn State. In Proceedings of the IEEE OCEANS 2003, San Diego, CA, USA, 22–26 September 2003; Volume 5, pp. 2607–2610.
41. Johnson, D.H.; Dudgeon, D.E. *Array Signal Processing: Concepts and Techniques*; Simon & Schuster: New York, NY, USA, 1992.
42. Oppenheim, A.V.; Willsky, A.S.; Nawab, S.H. *Signals and Systems*; Prentice-Hall: Englewood Cliffs, NJ, USA, 1983; Volume 6, p. 10.
43. Wang, D.; Ratilal, P. Angular Resolution Enhancement Provided by Nonuniformly-Spaced Linear Hydrophone Arrays in Ocean Acoustic Waveguide Remote Sensing. *Remote Sens.* **2017**, *9*, 1036. [CrossRef]
44. Makris, N.C.; Avelino, L.Z.; Menis, R. Deterministic reverberation from ocean ridges. *J. Acoust. Soc. Am.* **1995**, *97*, 3547–3574. [CrossRef]
45. Ratilal, P.; Lai, Y.; Symonds, D.T.; Ruhlmann, L.A.; Preston, J.R.; Scheer, E.K.; Garr, M.T.; Holland, C.W.; Goff, J.A.; Makris, N.C. Long range acoustic imaging of the continental shelf environment: The Acoustic Clutter Reconnaissance Experiment 2001. *J. Acoust. Soc. Am.* **2005**, *117*, 1977–1998. [CrossRef] [PubMed]
46. Jain, A.D. Instantaneous Continental-Shelf Scale Sensing of Cod With Ocean Acoustic Waveguide Remote Sensing (OAWRS). Ph.D. Thesis, Massachusetts Institute of Technology, Cambridge, MA, USA, 2015.
47. Sezan, M.I. A peak detection algorithm and its application to histogram-based image data reduction. *Comput. Vis. Gr. Image Process.* **1990**, *49*, 36–51. [CrossRef]
48. Tran, D.; Andrews, M.; Ratilal, P. Probability distribution for energy of saturated broadband ocean acoustic transmission: Results from Gulf of Maine 2006 experiment. *J. Acoust. Soc. Am.* **2012**, *132*, 3659–3672. [CrossRef] [PubMed]
49. Makris, N.C. The effect of saturated transmission scintillation on ocean acoustic intensity measurements. *J. Acoust. Soc. Am.* **1996**, *100*, 769–783. [CrossRef]
50. Shapiro, A.D.; Wang, C. A versatile pitch tracking algorithm: From human speech to killer whale vocalizations. *J. Acoust. Soc. Am.* **2009**, *126*, 451–459. [CrossRef] [PubMed]
51. Baumgartner, M.F.; Mussoline, S.E. A generalized baleen whale call detection and classification system. *J. Acoust. Soc. Am.* **2011**, *129*, 2889–2902. [CrossRef] [PubMed]
52. Kanungo, T.; Mount, D.M.; Netanyahu, N.S.; Piatko, C.D.; Silverman, R.; Wu, A.Y. An efficient k-means clustering algorithm: Analysis and implementation. *IEEE Trans. Pattern Anal. Mach. Intell.* **2002**, *24*, 881–892. [CrossRef]
53. Duda, R.O.; Hart, P.E.; Stork, D.G. *Pattern Classification*; John Wiley & Sons: New York, NY, USA, 2012.
54. Gong, Z.; Ratilal, P.; Makris, N.C. Simultaneous localization of multiple broadband non-impulsive acoustic sources in an ocean waveguide using the array invariant. *J. Acoust. Soc. Am.* **2015**, *138*, 2649–2667. [CrossRef] [PubMed]
55. Urick, R. *Principles of Underwater Acoustics*; McGraw-Hili Inc.: New York, NY, USA, 1975.
56. Kinsler, L.E.; Frey, A.R.; Coppens, A.B.; Sanders, J.V. Fundamentals of acoustics. In *Fundamentals of Acoustics*, 4th ed.; Kinsler, L.E., Frey, A.R., Coppens, A.B., Sanders, J.V., Eds.; Wiley-VCH: New York, NY, USA, 1999; p. 560, ISBN 0-471-84789-5.
57. Jensen, F.B.; Kuperman, W.A.; Porter, M.B.; Schmidt, H. *Computational Ocean Acoustics*; Springer Science & Business Media: New York, NY, USA, 2000.
58. Fonseca, J.M.; Moura-Pires, F. Ship noise evaluation based on segmented decision trees. In Proceedings of the 1992 lEEE/RSJ International Conference on Intelligent Robots and Systems, Raleigh, NC, USA, 7–10 July 1992; Volume 3, pp. 1823–1828.
59. Chen, J.; Li, H.; Tang, S.; Sun, J. A SOM-based probabilistic neural network for classification of ship noises. In Proceedings of the IEEE 2002 International Conference on Communications, Circuits and Systems and West Sino Expositions, Chengdu, China, 29 June–1 July 2002; Volume 2, pp. 1209–1212.

60. Farrokhrooz, M.; Karimi, M. Ship noise classification using probabilistic neural network and AR model coefficients. In Proceedings of the IEEE Oceans 2005-Europe, Brest, France, 20–23 June 2005; Volume 2, pp. 1107–1110.
61. Xi-ying, H.; Jin-fang, C.; Guang-jin, H.; Nan, L. Application of BP neural network and higher order spectrum for ship-radiated noise classification. In Proceedings of the 2010 2nd International Conference on Future Computer and Communication (ICFCC), Wuhan, China, 21–24 May 2010; Volume 1, pp. V1–712.
62. De Robertis, A.; Handegard, N.O. Fish avoidance of research vessels and the efficacy of noise-reduced vessels: A Review. *ICES J. Mar. Sci.* **2012**, *70*, 34–45. [CrossRef]